EVALUATION OF ACID FRACTURING BASED ON THE "ACID FRACTURE

NUMBER" CONCEPT

A Thesis

by

ABDULWAHAB ALGHAMDI

Submitted to the Office of Graduate Studies of
Texas A&M University
in partial fulfillment of the requirements for the degree of

MASTER OF SCIENCE

May 2006

Major Subject: Petroleum Engineering

EVALUATION OF ACID FRACTURING BASED ON THE "ACID FRACTURE

NUMBER" CONCEPT

A Thesis

by

ABDULWAHAB ALGHAMDI

Submitted to the Office of Graduate Studies of
Texas A&M University
in partial fulfillment of the requirements for the degree of

MASTER OF SCIENCE

Approved by:

Chair of Committee,   Peter Valko
Committee Members,   Stephen A. Holditch
                                     Wayne Ahr
Head of Department,   Stephen A. Holditch

May 2006

Major Subject: Petroleum Engineering

ABSTRACT

Evaluation of Acid Fracturing Based on the "Acid Fracture

Number" Concept. (May 2006)

Abdulwahab Alghamdi, B.S., King Fahd University of

Petroleum and Minerals, Dhahran-Saudi Arabia

Chair of Advisory Committee: Dr. Peter Valko

Acid fracturing is one of the preferred methods to stimulate wells in carbonate reservoirs. It consists of injecting an acid solution at high enough pressure to break down the formation and to propagate a two-wing crack away from the wellbore. The acid reacts with the carbonate formation and this causes the etching of the fracture surfaces. After the treatment, the created etched surfaces do not close perfectly and that leaves behind a highly conductive path for the hydrocarbons to be produced. We distinguish the issue of treatment sizing (that is the determination of the volume of acid to be injected) and the issue of creating optimum fracture dimensions given the size of the treatment. This is reasonable because the final cost of a treatment is determined mainly by the volume of acid injected and our goal should be to achieve the best performance of the treated well. The well performance depends on the created fracture dimensions and fracture conductivity and might change with time due to various reasons.

This research evaluates two field cases from Saudi Aramco where acid fracturing treatment has been used to stimulate a carbonate formation. I investigated the following

issues: a) how effective was the treatment to restoring the initial productivity, b) how did the productivity of the well change with time; c) what are the possible reasons for the change in performance, d) what are our options to improve acid fracture design in the future?

Based on our research work both near-well liquid drop-out and fracture-conductivity deterioration can impact the production in different proportion. Moreover, the fracturing model tends to overestimate the fracture conductivity in some cases as shown in SA-2. Also, the "Acid fracture Number" concept proves to be an effective way to evaluate the acid fracturing treatment. Several recommendations were made based on this research work as described in the last part of my thesis.

DEDICATION

This work is dedicated

To my parents for encouraging me to achieve this goal;

To my beloved wife, I want to say I love you Balqees and finally we can celebrate this

achievement together;

To all my brothers and sisters, Thanks for all you did for me and wishing you all good

health.

ACKNOWLEDGEMENTS

TABLE OF CONTENTS

Page

LIST OF FIGURES

FIGURE   Page

LIST OF TABLES

TABLE   Page

CHAPTER I

INTRODUCTION

Acid fracturing is one of the fundamental ways to stimulate a well completed in a carbonate reservoir. The two main processes incorporated with acid fracturing are the etched fracture conductivity and the acid penetration distance. In a heterogeneous formation, acid fracturing has proved to be a successful method to enhance hydrocarbon recovery. Moreover, in a tight-gas reservoir, acid fracturing become the most economical method to produce the gas reservoir[1]. Much research has been done to study acid penetration in acid fracturing.

The acid fracturing treatment data sets which were evaluated in this study were obtained from Saudi Aramco Oil Company. These treatments were performed on wells located in the giant Ghawar field. In the next section, I will describe the reservoir geology and I will define some of the critical parameters which affect the fracture geometry.

1.1 Reservoir Geology

The Ghawar structure is located in the eastern region of Saudi Arabia. This gigantic field stretches over a 225 km x 25 km (140 miles x 15 miles) and produces gas from its Pre-Khuff and Khuff carbonate reservoirs (see **Fig. 1.1**).

_____

This thesis follows the style of *SPE Journal*.
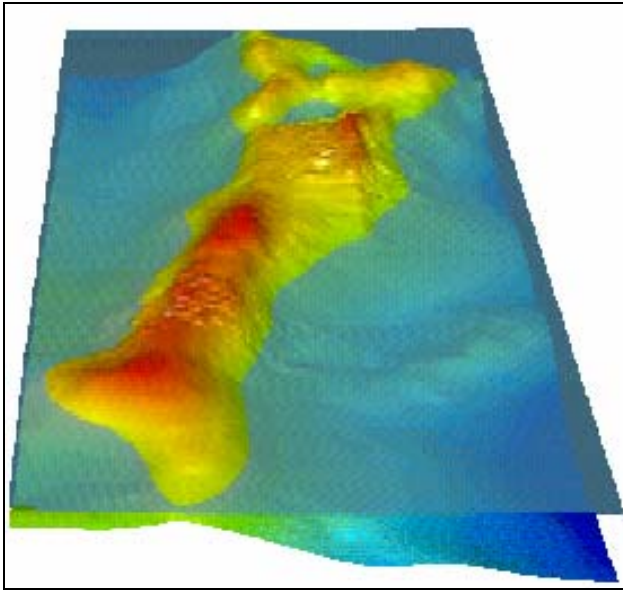
Fig. 1.1-Ghawar field structure (after Rahim).[1]

The distribution of sour gas and condensate content in the gas varies from one location to another in the same field. A typical Khuff well produces from approximately 15 – 30 m (50 – 100 ft) of net pay. The Khuff reservoirs are predominantly calcite and dolomite, interbedded with anhydrite in concentrations up to 15 wt% in the tighter sections.[2] Within the same section, there is a variation in formation lithology.

1.2   Khuff Formation

The Khuff formation is a deep gas carbonate reservoir that consists of dolomite and limestone sections in the eastern region of Saudi Arabia. The Khuff formation is an ideal candidate for acid fracturing because of the heterogeneous nature of the formation, which tends to help create the needed fracture conductivity.[3] However, the variation in the fracture degree (fracture geometry), loss circulation while drilling, and early water breakthrough are a few among the most common problems encountered in these reservoirs.[4,5]

The Khuff and Pre-Khuff are deep gas condensate reservoirs is an active tectonic stress environment.[1] This formation belongs to the late Permian age and lies between 11,000 and 12,000 ft. The Khuff formation is subdivided into four main zones, denoted as A, B, C, and D. The two main producing intervals of this reservoir are Khuff B and Khuff C. Both reservoirs tested and proved to have a high quantity of condensate rich gas. The average pay thickness in each reservoir estimated to be 110 ft and 180 ft for both Khuff B and Khuff C respectively.[6]

The next section summarizes some of the critical parameters and their impact on fracture geometry.

1.2.1 In-Situ Stress

An important mechanical property in fracture treatment design is the in-situ stress. In-situ stress impacts mainly the vertical and lateral growth of the fracture, and shapes the overall fracture dimensions. Several methods[1] can be used to calculate the in-situ stress profile. These techniques include over-coring, analysis of focal mechanisms of induced seismicity, size of borehole breakouts, core relaxation and Keiser effect.[7,8] In the given field cases that I am going to evaluate in this study, the in-situ stress estimated by the most dependable method of calculating in-situ stress which is analyzing field pressure data from Microfrac and Minifrac treatments where fluid is pumped at a rate to barely create a fracture. The pumps are then shut down to measure the initial pressure drop (ISIP) and pressure drop with time as shown in **Figure 1.2**. Nolte's analysis or history matching technique is then used to determine fracture closure. In the Khuff formation

the in-situ stress measured to be 10,000 to 11,000 psi. Also, the vertical stress gradient across the Khuff reservoir estimated to be 1.1 psi/ft across the Khuff reservoir.[7,8]
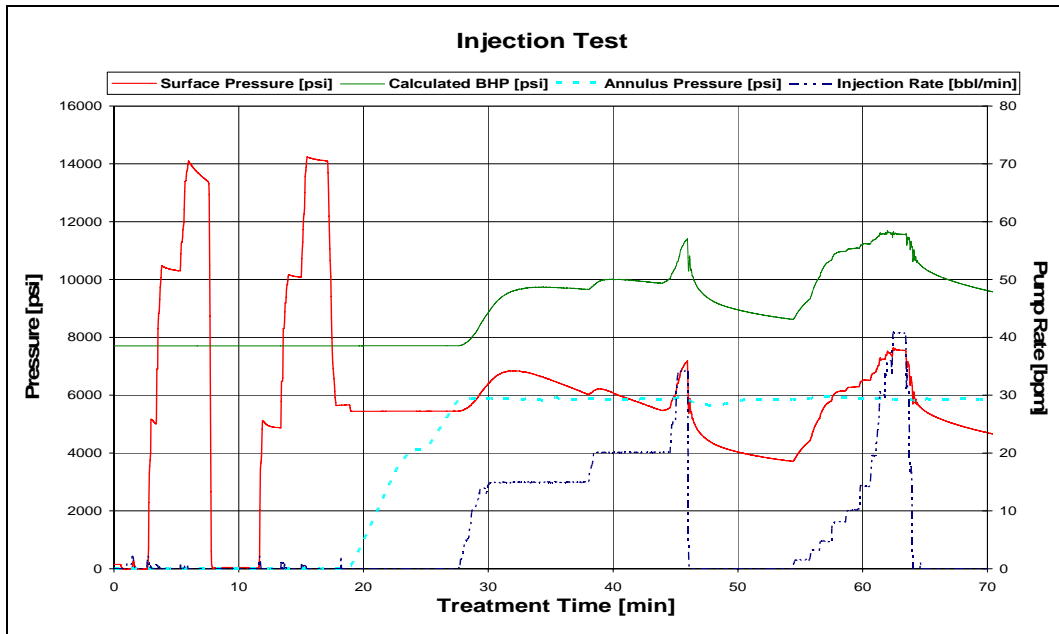
Fig. 1.2- Fracture presuure history match for SA-1.

1.2.2   Young's Modulus

Young's modulus, E, is the ratio of applied stress to the longitudinal strain. It can be interpreted as the rock "stiffness," or a parameter expressing the resistance of the rock to deform under a given tensional or compressional loading condition. Young's modulus is an important property that impacts the fracture geometry. Narrow fractures are created in formation with high modulus; whereas wide fractures are created in low modulus formations. The treatment must be carefully designed when high modulus values are encountered to avoid possible breakthrough into undesired intervals as the fracture have

a high tendency to create tall fracture.[1,9] In the Khuff formation, the Young's modulus vary between 4E+6 and 9E+6 psi.

1.2.3 Poisson's Ratio

Poisson's ratio, υ, is the ratio of the lateral strain to the longitudinal strain. It represents the amount that the sides of a cube or core plug bulge out when the top is compressed. Poisson's ratio is always positive and less than 0.5. [1,10] The Khuff formation has Poisson's ratio that ranges from 0.25 to 0.35.

1.2.4 Formation Permeability

The permeability reflects the ability of gas to flow within a formation. High permeability formations are more susceptible to formation damage during drilling, and may only require a matrix acid treatment for cleanup. In a low to moderate permeability reservoir, long fractures are required to effectively increase the productivity index. On the other hand, a short and conductive fracture might be best for a high permeability reservoir. As mentioned earlier the Khuff reservoirs are very heterogeneous formation and since it have average permeability of 0.5 – 4.0 md which suggested the second choice.[7] The Khuff reservoirs have significant but variable porosity ranged from 0 to 35%.

1.2.5 Reservoir Pressure

Reservoir pressure affects the volume of hydrocarbon reserves, and the ability to flow back and cleanup the fracturing fluids after the treatment. The choice of fracturing fluid and also the success of a treatment can largely depend upon the reservoir pressure. The

average initial reservoir pressure in the khuff reservoir is 7,500 psi and the average

bottomhole temperature is 275°F.

1.2.6 Fluid Leakoff Coefficient

The total fluid loss coefficient can be approximated with the following equation[10]

$$C_t = 0.047 (\frac{\Delta p \phi k}{\mu})^{0.5}$$ ……………………………………………………………………..1.1

Where C_t is the total fluid loss coefficient and Δp is the pressure difference between the

fluid in the fracture and in the formation. Better reservoir quality (porosity, permeability,

pay thickness) increases fluid loss. The best method to compute C_t is through history

matching minifracture treatments prior to pumping the actual treatment.

To control leakoff, industry has been using emulsions and acids gelled with

polymers. Polymers are the most widely used because of its stability at high bottomhole

temperature, especially in the presence of acid due to hydrolysis. Many carbonate

formations contain micro-fractures ($\sim 5 \times 10^{-4}$ inch wide) and during acid fracturing, leak-

off occurs through these micro-fractures as well as through the matrix. [11] Acid can

increase the permeability of these fractures several thousand-fold and the leak-off

control is always a challenge. The fluid-loss could be controlled to some extent by the

use of alternating stages of pad fluids and acids.[11]

The reaction of HCl with carbonate formations is fast, especially at high

temperatures. This means that the acid will not be able to penetrate deeply down the

fracture, which may affect the outcome of acid fracturing treatments. Polymers with and

without cross-linkers can be used to reduce the rate of acid reaction with carbonate.

Nasr-El-Din and coworkers[12] reported lab results that indicated the polymer can be trapped in the wormholes and the crosslinker, especially iron, can precipitate in sour environments.[12]

The pad fluid that was used in these treatments were mainly viscoelastic surfactant fluids. The system is made by mixing a specific surfactant with HCl. Depending on the job requirement, the acid concentrations can vary from 5 to 28 wt% HCl. The VES-AC has low viscosity at surface conditions. The HCl present in the system reacts with the calcite as shown in **Equation 1.2**, or dolomite as shown in **Equation 1.3**. The by-products of the reaction are $CaCl_2$, $MgCl_2$, CO_2 and H_2O.

Calcite:

$$CaCO_3 + 2\ HCl \rightarrow CaCl_2 + CO_2 + H_2O \dots\dots\dots\dots\dots\dots\dots\dots\dots\dots\dots\dots\dots\dots\dots\dots 1.2$$

Dolomite:

$$CaMg(CO_3)_2 + 4HCl \rightarrow CaCl_2 + MgCl_2 + 2CO_2 + 2H_2O \dots\dots\dots\dots\dots\dots\dots\dots 1.3$$
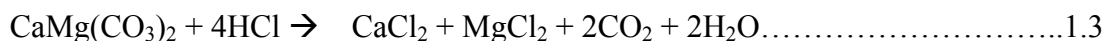
The $CaCl_2$ that is produced as the acid spends will react with the surfactant in-situ to form a viscous gel. This increased in the viscosity will continue as the acid spends which will help to further minimize leak-off. In general, the viscoelastic surfactant works by itself without additives. However, Corrosion inhibitor is still needed to protect the tubing string. AbdulWahab et al.[13] show that the corrosion inhibitor does not affect the viscosity of the VES system. The current application of the VES system include continuously injected of surfactant during pumping of the inert and acid fluids. This mixing procedure eliminates tank-bottom and the disposal of unused fluids. The use of

this mixing and pumping system will thus allow saving time and minimizing environmental impact.[11]

1.2.7   Embedment Strength

Rock embedment strength is defined[14] as the force required to push a steel ball bearing into the rock surface to a distance equal to the radius of the ball, divided by the projected area of the bearing. Higher embedment strength value indicates more competent rock. Embedment strength is measured in the laboratory and can vary between 30,000 psi to over 100,000 psi in the Khuff formation.[15]

Nasr-El-Din *et al.*[15] made measurements on the Khuff formation using Brinellhardness (BH) methods before and after exposure to acid. Rock strength was reduced by 20 to 63 % after acidizing as shown in **Table 1.1**. The dolomite sample that was reduced 63 % was due to a higher degree of porosity and permeability from vugs. However, in my research work, I used the embedment stress as an average value of 100,000 psi considering the value needed for Nierode-Kruk correlation is the rock property before the acid reaction. Also I used 50,000 psi to see how the results would change.

TABLE 1.1-HARDNESS INFORMATION BEFORE AND AFTER ACIDIZING KHUFF CORE SAMPLES (AFTER NASR-EL-DIN).[15]		
Lithology	Rock Embedment Strength, psi	
	Before	After
Limestone	70,425	50,784
	51,072	31,494
	59,041	39,040
Dolomite	62,027	49,324
	129,988	47,647

1.3   Objectives

The objective of my thesis is to evaluate two field cases from Saudi Aramco where acid fracturing treatment has been designed and pumped. In this study we investigated the following issues: a) how effective was the treatment to restoring the initial productivity, b) how did the productivity of the well change with time; c) what are the possible reasons for the change in performance, and d) what are our options to improve acid fracture design in the future?

1.4   Organization of Thesis

My thesis includes seven chapters (I, II, II, …..and VII):

Chapter I presents the reservoir geology and the critical parameters which affect the fracture geometry. The other chapters organized as the following:

Chapter II presents the theory and the methodology I used in my calculation.

Chapter III summaries the field cases with the well description.

Chapter IV presents the fracture mechanism and the including the acid fracture program and the fluid system that was used.

Chapter V presents the evaluation part for the fracture geometry, bottomhole pressure, effective fracture conductivity and productivity index analysis

Chapter VI discus the reasons of the production behavior and the possibility of proppant as an alterative.

Chapter VII presents summary, conclusions, and some recommendation for Saudi Aramco Oil company to assist their acid fracturing program.

Finally, I present the nomenclature, references, and three appendixes developed in this research.

CHAPTER II

THEORETICAL BACKGROUND

The creation of hydraulic conductivity created by acid etching was not fully understood for many years. One of the main concerns of scientists over the years has been to develop a method to calculate the expected fracture conductivity for an acid fracturing treatment. To design the optimal treatment, we have to be able to estimate the etched fracture length and the effective fracture conductivity as a function of the volume of the acid pumped down the fracture. In this study, I used the available correlation to estimate the fracture conductivity as part of my evaluation.[14]

A new application has also been developed in this study to apply the proppant number concept which was developed by Valko and Economides[16,17,18] to acid fracture design and evaluation . The same concept can be applied by introducing the acid fracture number instead of the proppant fracture number.

In this chapter, I will discuss the theory behind the methodology I followed in my research starting by defining the dimensionless productivity index, and how it is related to the acid fracture number concept. Also, I will support the concept I applied to calculate both the flowing bottomhole pressure and the change in the fracture conductivity with time. Then, I will describe the gas well performance calculation. Finally, I will define the treatment evaluation methodology I used to investigate the change in the productivity index with time.

2.1   Dimensionless Productivity Index

One method to evaluate the performance of a well is to calculate the productivity index which is simply the production rate divided by the pressure drawdown

$$PI = \frac{q}{\bar{p} - p_{wf}} \quad \text{...2.1}$$

However, for a gas well equation (1) become,

$$PI = \frac{q\mu z}{p^2 - p_{wf}^2} \quad \text{...2.2}$$

The dimensionless productivity Index J_D is defined as

$$J_D = \frac{\alpha_1 B\mu}{kh} PI \quad \text{..2.3}$$

Similarly, for natural gas wells, J_D is

$$J_D = \frac{\alpha_2 \mu ZT}{kh} PI \quad \text{..2.4}$$

Later on we will see more details about the gas well performance and the use of J_D in that calculation.

The dimensionless productivity index, J_D depends on two dimensionless parameters: the dimensionless fracture conductivity, C_{fD} and the penetration ratio, I_x

C_{fD} is given by:
$$C_{fD} = \frac{(kw)_{af}}{kx_f} \quad \text{...2.5}$$

and the penetration ratio is

$$I_x = \frac{2x_f}{x_e} \quad \text{..2.6}$$

Valko and Economides[17,18] represent the above two dimensionless groups by introducing new dimensionless variable called N_{prop} .Similarly, N_{af} can be used in the case of acid fracture.

Hence,

$$N_{af} = I_x^2 C_{fD} = \frac{4x_f(kw)_{af}}{kx_e^2} = \frac{4x_f(kw)_{af}h_p}{kx_e^2 h_p} \dots\dots\dots\dots\dots\dots\dots\dots\dots\dots\dots\dots\dots\dots2.7$$

Where $(kw)_{af}$ is described as the effective conductivity of the created acid fracture.

Therefore, at a given N_{af} and C_{fD}, the dimensionless productivity index can be determined using the chart developed by Valko and Economides. **Figures 2.1** and **2.2** can be used if both N_{Ac} and C_{fD} have been calculated.
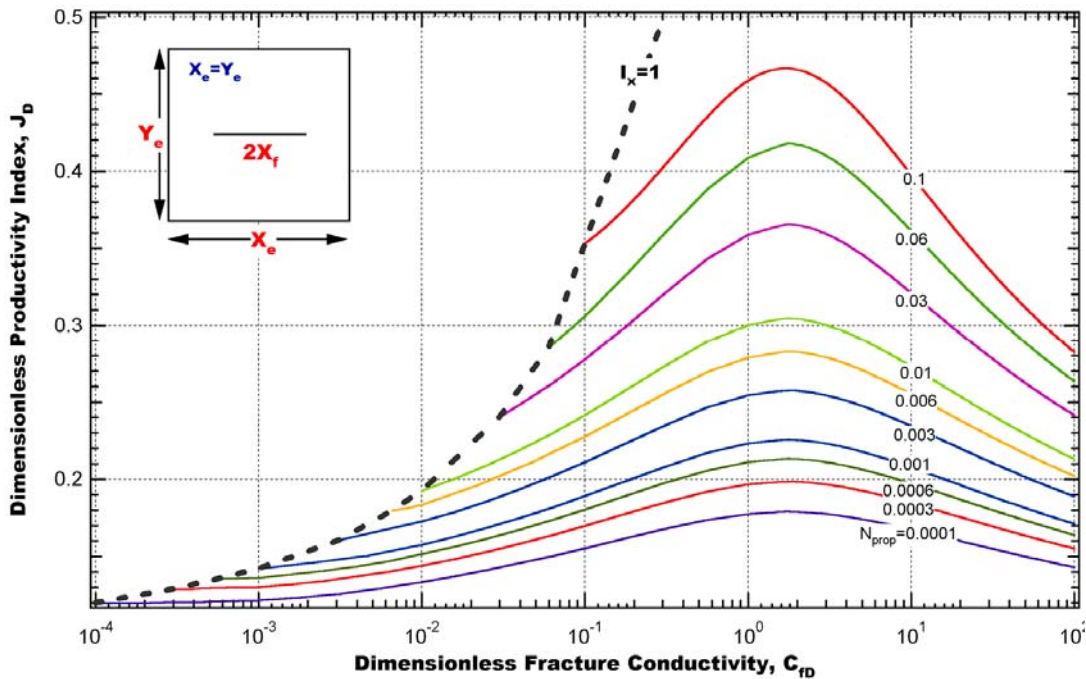
Fig. 2.1-Fracture performance as a function of dimensionless fracture conductivity for low acid number. Reproduced from SPE paper 73758.[18]
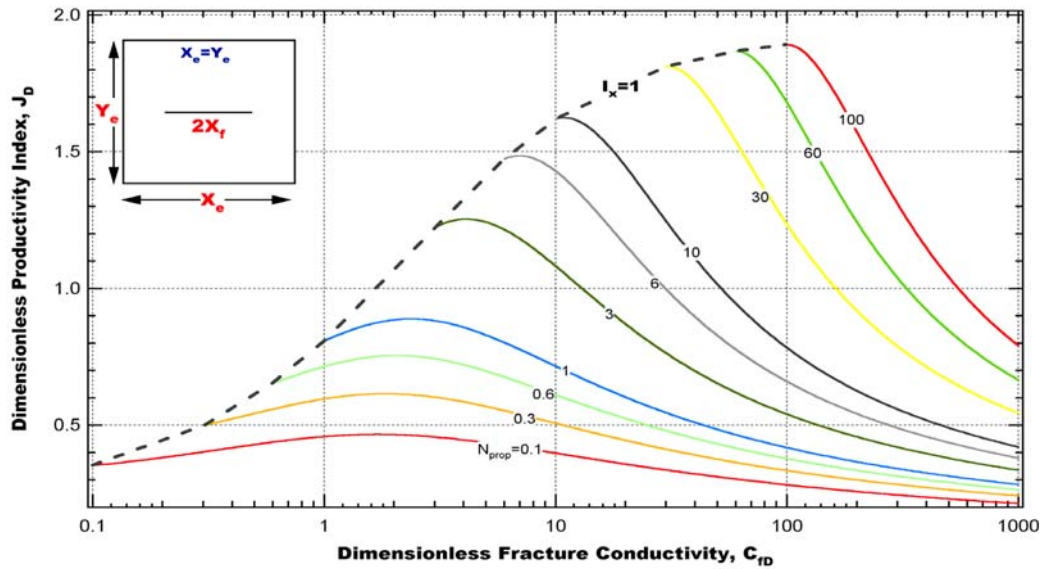
Fig. 2.2-Fracture performance as a function of dimensionless fracture conductivity for moderate\high acid number. Reproduced from SPE paper 73758.[18]

2.2   Flowing Bottomohole Pressure Calculation

Since I do not have a measure value for the FBHP for the field data cases I have evaluated in this research, I have computed the values using surface pressure and nodal analysis. The traditional way of solving the problem can be done graphically as shown in **Figure 2.3**. The graph is a combination of inflow performance relationship (IPR) and vertical lift performance (VLP).
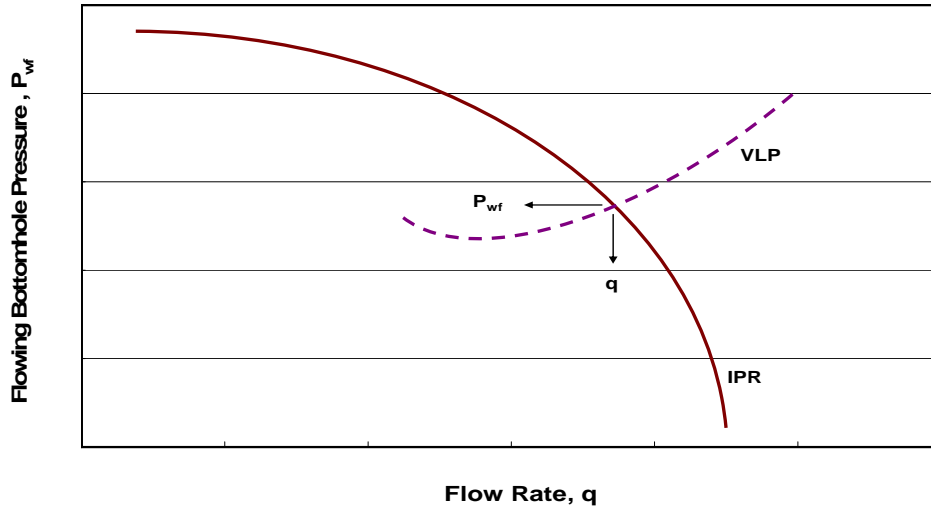
Fig. 2.3-Hypothetical case for combination of inflow performance relationship (IPR) and vertical lift performance (VLP).

For a single-phase flow of a compressible gas, **Equation 2.8[19]** represents the VLP.

$$p_1^2 = e^{-s} p_2^2 - 2.685 \times 10^{-3} \frac{f_f (ZTq)^2}{\sin \theta D^5} (1 - e^{-s}) \quad \dots\dots\dots\dots\dots\dots\dots\dots\dots\dots\dots\dots\dots\dots 2.8$$

The unknown pressure is the upstream pressure P_1.

Where s,

$$s = \frac{-0.0375 \gamma_g \sin \theta L}{ZT} \quad \dots\dots\dots\dots\dots\dots\dots\dots\dots\dots\dots\dots\dots\dots\dots\dots\dots\dots 2.9$$

However, there are many simulation models that can do such calculations. In this study PERRFORM[27] model (see **Chapter V**) was used to calculate the FBHP.

2.3   Nierode and Kruk[14] Correlation

The hydraulic conductivity created by acid etching is not totally understood. An empirical correlation for evaluating acid fracture conductivity was published by Nierode and Kurk over 20 years ago.[14] To calculate the acid fracture number, the effective

fracture conductivity needs to be calculated. The fracture conductivity after the acid fracture treatment can be obtained directly from the fracturing model or can be estimated by using Nierode and Kruk correlation.

In the Nierode-Kruk correlation, the acid fracture conductivity is expressed as a function of ideal fracture width, which is determined from the amount of rock dissolved, the rock embedment strength and the closure stresses

We first compute the ideal width

$$w_i = \frac{XV}{(1-\phi)\, 2\, h_f\, x_f}$$ 2.10

Then, we determine the effective fracture conductivity of the acid fracture from the ideal width, taking into account an additional formation strength parameter (rock embedment strength) and the net closure stress acting on the fracture faces.

$$k_f w = C_1 e^{-C_2 \sigma}$$ 2.11

$$C_1 = 1.47 \times 10^7 w_i^{2.47}$$

$$C_2 = (13.9 - 1.3 \ln S_{rock}) \times 10^{-3} \ \text{ if } S_{rock} < 20{,}000 \ \text{psi}$$

$$C_2 = (3.8 - 0.28 \ln S_{rock}) \times 10^{-3} \ \text{ if } S_{rock} > 20{,}000 \ \text{psi}$$

Figure 2.4 shows a Hypothetical diagram for the net closure stress which is a result of the minimum horizontal stress against the fracture opening face control be flowing botomhole pressure
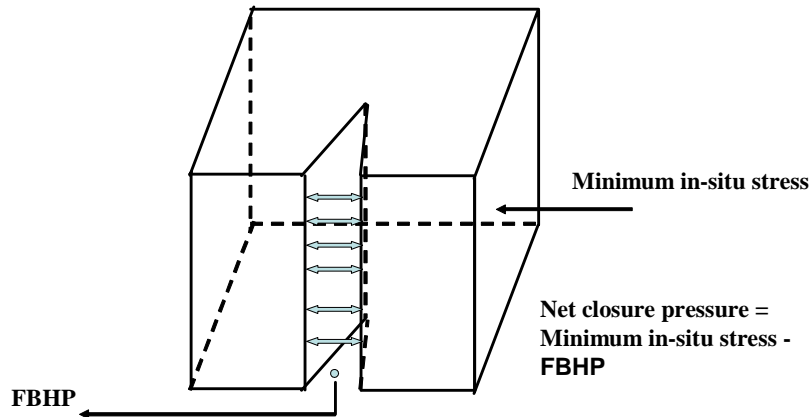
Fig. 2.4-Hypothetical diagram indicates the physical meaning of the net closure stress which was used in Nierode-Kruk correlation.

The experimental studies show that the effect of rock heterogeneity is very important. However, the Nierode-Kruk correlation resulting from homogeneous rough walled and in case of rock heterogeneity the value can underestimate by this correlation due to the small sample size but the correlation still practical.

Recently, Gong *et al.*[20] made an important advance by developing a new correlation to predict the acid fracture conductivity where the roughness and the asperity of the rocks after acidizing were taken into account. Based on their experimental results, a new fracture deformation model was derived which considers both the surface roughness and the rock mechanical properties. Gong found that Acid fracture conductivity is affected by the aperture and the contact area of the fracture under closure stress. This in turn, depends on the surface asperities created by the acidizing process and the mechanical strength of these asperities. Also he showed that acid contact time, acid leakoff, rock mechanical properties and formation heterogeneity all affect the creation of hydraulic conductivity of an acid fracture.

Figure 2.5 shows a comparison between the Nierode-Kruk correlation and the new model done by Gong.[20] The results showed the new model agreed well with the measured conductivity, while the Nierode-Kruk correlation tended to over predict the conductivity at higher closure stress for different acidizing conditions. However, the new model needs measurement of the surface roughness distribution after acidizing. Part of my research is to calculate the theoretical fracture conductivity but since this information is not available in my case, I will use the Nierode-Kruk correlation to calculate the acid fracture conductivity.
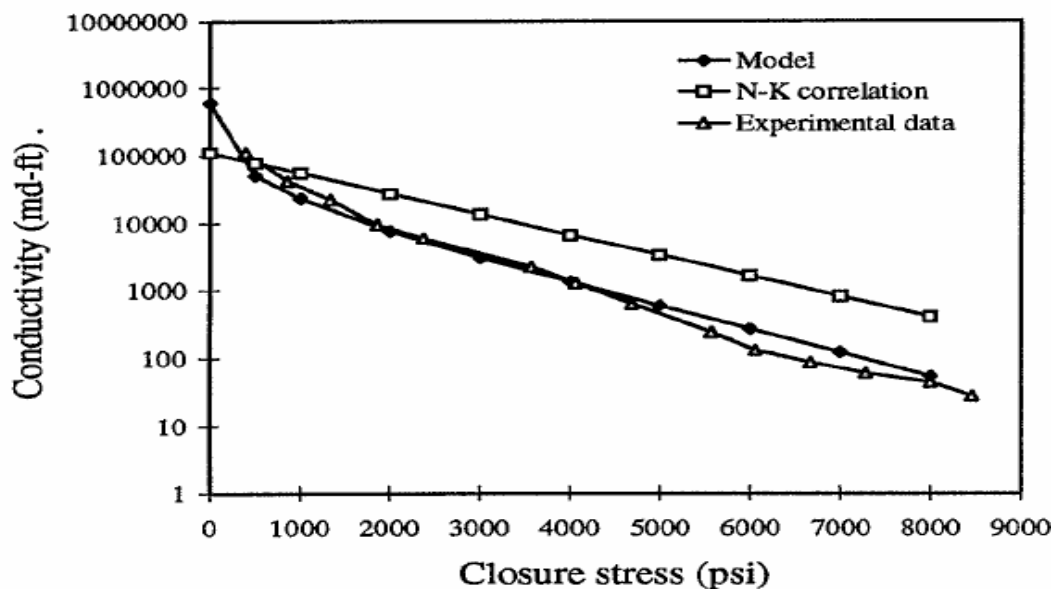
Fig. 2.5-Comparison between Gong model and Nierode-Kruk correlation. Reproduced from SPE paper 39431.[20]

Nierode-Kruk[14] correlation was based on the principle that the larger the amount of rock etched, the larger the conductivity of the fracture. However, Gong et al.[20] concluded that longer exposure times to HCl yielded more etching and higher conductivity. Navarrete[21] has another point of view he said:

"This also leads to an inefficient use of the acid that tends to excessively spend at the wellbore, resulting in poor conductivity closer to the tip of the fracture. On the other hand, if the reaction rate is too slow, the amount of rock dissolved may be insufficient to prevent fracture closure."

"Although the most reactive system created 32 times more fracture volume, once closure stress was applied it did not result in higher conductivities. This suggests that it is more efficient to have the acid spend more uniformly along the fracture axis (emulsified acid) than mostly at the entrance. The added benefit of controlled acid spending is preservation of acid strength to generate longer fracture length. These results indicate that more fracture volume does not necessarily translate into higher conductivities."

2.4   Gas Well Performance[19]

For Pseudo-steady state and assuming Darcy flow, the gas flow rate, q (MSCF/d) can be estimated by using **Eqn.2.12** and solving for q:

$$p_{avg}^2 - p_{wf}^2 = \frac{1424 q \mu z T}{kh} \frac{1}{J_D} \dots\dots\dots\dots\dots\dots\dots\dots\dots\dots\dots\dots\dots\dots\dots\dots\dots\dots\dots\dots2.12$$

The cumulative production from a gas reservoir, considering the expansion of the fluid is

$$\dots\dots\dots\dots\dots\dots\dots\dots\dots\dots\dots\dots\dots\dots\dots\dots\dots\dots\dots\dots\dots\dots\dots\dots2.13$$

$$G_p = G_i - \left(1 - \frac{\frac{p_{avg}}{z}}{\frac{p_i}{z_i}}\right)$$

Where z and z_i are the corresponding gas deviation factor at a given pressure and temperature

To compute G_i; $$G_i = \frac{Ah\phi S_g}{B_{gi}} \dots\dots\dots\dots\dots\dots\dots\dots\dots\dots\dots\dots\dots2.14$$

The gas formation factor B_{gi}, can be estimated by:

$$B_{gi} = 0.0283 \frac{ZT}{P}$$ 2.15

By using **Equations. 2.12 to 2.15,** one can develop a forecast for a gas well performance versus time until the average reservoir pressure declines to certain value depending on the available production data.

Another parameter to calculate is the time required to transition to pseudo-steady state from infinite acting behavior, which can be calculated by

$$t_{pss} = 1200 \frac{\phi \upsilon c_t r_e^2}{k}$$ 2.16

2.5 Treatment Evaluation Methodology Based on the Acid Fracture Number

According to the fracture number concept, the productivity index can be calculated if both dimensionless fracture conductivity and acid fracture number estimated. To answer the question regarding the change in the productivity of the well with time, I approached this subject from two prospectives:

2.5.1 *Meathod (a)*

The design model (FracCADE) predicts the fracture geometry. In addition, the Nierode-Kruk method was used to estimate the change in fracture conductivity with time. Using **Equations 2.5** and **2.7,** the dimensionless fracture conductivity and acid fracture number can be calculated, respectively. From the charts given in **Figures 2.1** and **2.2**, one can calculate the nominal productivity index (or nominal skin).

2.5.2   Meathod (b)

The actual productivity index of the well can be calculated from the monthly production data coupled with the calculated values of flowing bottomhole pressure which were estimated by using a nodal analysis computer program. Our analysis is based on comparing the two results. The results obtained from method (a) are the theoretical productivity index and the results obtained from method (b) are the actual productivity index. **Figure 2.6** describes the two methods applied to describe the change in the productivity of the well with time.
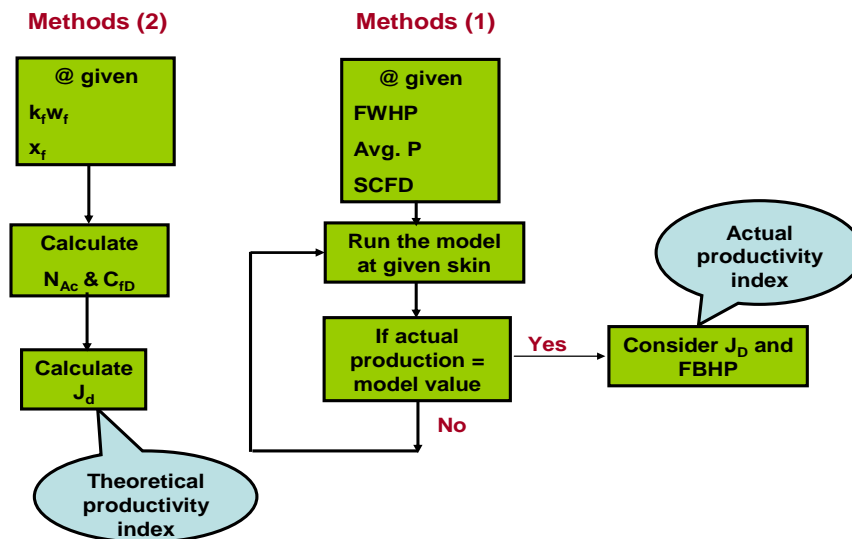
Fig. 2.6-Flow chart describes the two methods applied to describe the change in the productivity of the well with time.

CHAPTER III

FIELD CASES

Two field cases from Saudi Aramco where acid fracturing treatments have been pumped were evaluated in this study. In this chapter, I will describe the reservoir characteristics and the fracture geometry I consider important in my analysis. Also, the pumping schedule for the acid stages will be given for each case.

3.1 Well Description

Data from five acid fracture treatments have been received on wells SA-1, SA-2, SA-3, SA-4, and SA-5. The treated zones can be either Khuff-B or Khuff-C or a combination of both B and C as we will see in SA-3. However, we only had a production data for two of the wells.

3.1.1 Case Study-1: Well SA-1

SA-1 is gas well that was fracturedwith acid in the Khuff C zone. The well has two sets of perforations. The upper Khuff-C was perforated with 6 shots/foot between 11,400 and 11,525 ft. The lower Khuff-C was perforated from 11,525 to 11,575 ft with 1 shot/ft. The producing zones have permabilities ranging from 1.22 to 4.0 md, with an arithmetic average permeability of 2.21 md, while the porosity varies from 7.5 to 20 %. The reservoir data are summarized in **Table 3.1**.

TABLE 3.1-SA-1 RESERVOIR DATA							
Layer	Start of Interval	End of Interval	Thickness of interval	Permeability (md)	Porosity, %	Kh, (md-ft)	Sg, %
1	11,402	11,425	23	1.22	8	28.06	70
2	11,440	11,452	12	1.50	12	18.00	85
3	11,458	11,500	42	1.44	10	60.48	85
4	11,501	11,525	24	1.18	7.5	28.32	40
5	11,525	11,575	50	4.0	20	200.0	88

The bottomhole temperature was estimated to be 270°F. This well has a net pay of 151 ft. The mechanical properties of the rock include a Poisson ratio of 0.29, and a Young's modulus of 6.1E+6 psi. The average in-situ stress is 10,400 psi at ~10,850 ft and average reservoir pressure is 7,500 psi. The well has a gas with specific gravity of 0.79 and a drainage area of 2250 acres. Additional average reservoir data and other well characterization data are given in **Table 3.2**.

TABLE 3.2-SA-1 AVERAGE RESERVOIR DATA AND WELL CHARACTERIZATION					
Parameter	Value	Unit	Parameter	Value	Unit
Net pay	151.0	ft	Reservoir Temperature	270.00	oF
Permeability	2.22	md	Gas specific gravity	0.79	---
Growth thickness	173	ft	Reservoir pressure	7500	psi
Average porosity	11.5	---	Drainage area	2250	acre
Average gas saturation	73.6	---	In-Situ Stress	10,400	psi
Viscosity	0.035	cp	Bottomhole flow pressure	6,442	psi

Table 3.3 Summarizes the volumes of acid pumped into well SA-1.Details concerning the treatment are found in **Chapter IV**.

TABLE 3.3-PUMPING SCHEDULE FOR SA-1				
Stage Name	Slurry Rate (bbl/minute)	Pump Time (Minute)	Slurry Volume (bbl)	Acid Volume (gal)
Pad (polymer gel)/ Acid	48.5	9.3	451	16,879
Pad (polymer gel)/ Acid	58.4	7.4	432	16,172
Pad (VES)/ Acid	64.6	6.6	426	15,955
Pad (VES)/ Acid	67.4	8.9	599	22,447
Closed Fracture Acid	55.3	5	276	10,347

3.1.2   Case Study-2: Well SA-2

SA-2 is the second well we evaluated, and it was drilled to 11,377 ft depth and is completed in the Khuff-C zone. The permeability in this well ranges from 0.049 to 3.49 md. The porosity ranges from 6 to 18 %. This well was completed with 89 ft of perforations. The reservoir data are summarized in **Table 3.4**

TABLE 3.4-SA-2 RESERVOIR DATA						
Layer	Start of Interval	End of Interval	Thickness of interval	Permeability (md)	Porosity %	Kh, (md-ft)	Sg, %
1	11,377	11,387	10	3.49	17	34.9	85
2	11,389	11,398	9	1.28	10	11.52	78
3	11,400	11,430	30	0.84	8	25.2	76
4	11,460	11,470	10	3.88	18	38.8	80
5	11,502	11,532	30	0.49	6	14.7	75

This well has a bottomhole temperature of 250 ºF. The average reservoir pressure is 7,505 psi. The mechanical properties of the rock include a Poisson ratio of 0.28 and a Young's modulus of 5.5 E+6 psi. The average in -situ stress is 10,830 psi. The well has a gas with specific gravity of 0.79 and a drainage area of 2250 acre. Additional average reservoir date and other well characterization are given in **Table 3.5**.

TABLE 3.5-SA-2 AVERAGE RESERVOIR DATA AND WELL CHARACTERIZATION					
Parameter	**Value**	**Unit**	**Parameter**	**Value**	**Unit**
Net pay	89	ft	Reservoir Temperature	250	^{o}F
Permeability	1.4	md	Gas specific gravity	0.79	---
Growth thickness	155	ft	Reservoir pressure	7,505	psi
Average porosity	11.8	---	Drainage area	2250	acre
Average gas saturation	78.8	---	In-Situ Stress	10,830	psi
Viscosity	0.035	cp	Bottomhole flow pressure	5,917	psi

Table 3.6 Summarizes the volumes of acid pumped into well SA-2.

TABLE 3.6-PUMPING SCHEDULE FOR SA-2				
Stage Name	**Slurry Rate (bbl/minute)**	**Pump Time (Minute)**	**Slurry Volume (bbl)**	**Acid Volume (gal)**
Pad (polymer gel)/ Acid	38.9	9.8	381	11,207
Pad (polymer gel)/ Acid	45.8	8.3	380	11,176
Pad (VES)/ Acid	51.9	8.1	420	16,491
Pad (VES)/ Acid	51.7	8.3	429	16,833
Closed Fracture Acid	23.7	14.3	338	14,120

3.1.3   Case Study-3,4&5: Well SA-2,4&5

Appendix A includes the reservoir data, well characterization and the pumping schedule for the other study cases SA-3, 4, and 5.Well SA-3 was fractured in two acid fracturing treatments for Khuff-B and Khuff-C.

CHAPTER IV

PROCEDURE AND FLUIDS APPLIED FOR FRACTURING

A hydraulic fracture is created using hydraulic pressure to overcome the tensile strength of the rock and the minimum in-situ stress in the target formation. This force, as it overcomes the in-situ minimal horizontal stress, initiates a fracture perpendicular to the direction of the minimal stress. The effectiveness of any acid fracturing treatment depends on the effective fracture length and conductivity. The conductivity in an acid fracture treatment, in turn, will depend on the fluid loss, rock dissolution, and the damage associated with the treatment fluid.[11] Hydraulic fractures are usually considered near vertical and thus, its vertical plane aligns with the wellbore near the perforated portion of the well. However, since no wellbore is truly vertical, the fracture and the wellbore can easily deviated as the fracture height grows. The dimensions of vertical fractures depend on the geomechanical properties of the formation and excess pressure generated within the fracture. The main geomechanical property components that impact fracture propagation and geometry are the (1) minimum in-situ stress and (2) Young's modulus of the various rock layers that affect the fracture. Fracture vertical growth can be restricted if high stress difference is encountered between the interval fracture initiates and the intervals either above or below it. Both lateral and vertical fracture growths depend upon in-situ stress, net pressure, pumping fluid characteristics, and completion technique. Indeed, the location of perforation play an important role in determining fracture geometry and careful choice of perforations is needed for the success of a fracture treatment.[22,23,24]

4.1 Acid Fracturing Computer Program

The fracture treatment fluids proposed for an acid fracture treatment take into account the following consideration; fluids selected to minimize formation damage, maximize effective fracture length, and enhance clean up efforts by decreasing clean up time. To this end, a polymer gel system coupled with a high temperature (HT) Breaker was selected for initial two pad volumes. A viscoelastic surfactant, micellar-gel was proposed for the third pad fluid, and subsequent gelled-acid stages for the main treatment. The high temperature VES system is designed to provide viscous fluid-loss control during injection; however, it will break down easily to a low-viscosity fluid with dilution by water, hydrocarbon, or mutual-solvent breaker solutions. VES fluids typically provide grater than 95% of fracture permeability retained, compared to 20-60% for polymer-based systems as a result of the formation damage caused by polymer. To ensure rapid breakdown/dilution of the viscous gels, an overflush of water containing 10 vol% mutual solvent was pumped. Additionally, two stages of emulsified preceded the gelled-acid stages, to achieve additional acid penetration and provide greater effective length/area. A final closed fracture acid stage at 20 wt% HCL was pumped at the end of the job to etch the critical matrix which helped in removing any near well bore damage. Burgos[25] reported that the effect the CFA stage on final productivity is not clear from the pressure data.

Table 4.1 summarizes the sequences of the fracture treatment schedule that was implemented to perform the acid fracturing treatment. Also **Table 4.2** includes more detail s about the pumped volume.

TABLE 4.1-THE SEQUENCES OF THE FLUIDS STAGES	
Stage Fluids	**Acid Concentration**
Pre-Pad	No Acid
↓	↓
polymer gel	No Acid
↓	↓
Emulsified Acid	28 wt% HCl
↓	↓
(VES)/ Acid	28 wt% HCl
↓	↓
Closed Fracture Acid	28 wt% HCl
↓	↓
Over-Flush	No Acid

TABLE 4.2-PUMP SCHEDULE FOR SA-1						
Stage #	Stage Name	Slurry Volume (bbl)	Slurry Rate (bbl/min)	Pump Time (min)	Fluid Name	Fluid Volume (gal)
1	Hole fill	300	16.7	17.9	Water frac	12,576
2	Inc. rate	15	34.6	0.4	Water frac	630
3	Shutdown	0.0	0.0	0.0	Water frac	0
4	Step Rate	148.7	4.6	32.7	Water frac	6,259
5	Shutdown	0.0	0.0	0.0	Water frac	0.0
6	Prepad	47.6	26.5	1.8	Water frac	1,973
7	Pad	230.8	45.9	5.0	Polymer gel	9,695
8	SXE	452.4	48.5	9.3	Emulsified acid	18,997
9	Pad	180.9	54.8	3.3	Polymer gel	7,596
10	SXE	433.3	58.4	7.4	Emulsified acid	18,198
11	Pad	309.5	61.9	5.0	Polymer gel	12,996
12	VDA	428.6	64.6	6.6	VES / Acid	18,001
13	Clearfrac	214.3	65.3	3.3	VES gel	9,000
14	VDA	600.2	67.4	8.9	VES / Acid	25,210
15	O-flush 1	309.5	60.7	5.1	Water frac	13,000
16	CFA	278.3	55.3	5.0	Acid	11,713
17	O-flush 2	428.6	31.6	13.6	Water frac	17,991
18	Flush	294	12.0	24.6	Water frac	12,407

4.2   Fluid System

4.2.1   Initial Pad Volume

The purpose of initial pad volume is to

- Provide effective fracture extension by controlling leakoff.

- Cool down the formation to slow down the reaction rate.

- Create a wide and long fracture that will provide a conduit for the acid to flow into the reservoir.

- Saturate natural fractures and vugs to minimize acid leakoff.[11]

The pad volume is calculated to create the length required to optimize stimulation for a particular formation, as well as vertical coverage of all pay zones of interest. If the pad volume is not too small, the created fracture may not be long enough to generate the optimal production. On the other hand, excess pad volume will not increase etched fracture area, as acid may already be spent before it reaches all created fracture. In some cases, increased pad volume may damage the formation. After performing several treatments with over forty thousand gallons of initial pad volume, the recommendation brought by Saudi Aramco engineers was to pump about 15,000 gallons of pad. This change in volume reduces the cost of acid fracturing while it does not compromise with the effectiveness of the treatments.[26] When acid is used without a pad fluid, the fracture will generally be short and narrow since the fluid loss for acid is high.

4.2.2 Acid Strength and Volume

The early development of the acid fracturing program consisted of pumping a viscous pad which is a combination of polymer and VES followed by 28% HCl. This type of design was an attempt to create fingering of the acid in the pad stages. Acid volumes of 28% HCl typically ranged from 1,500 - 2,000 gals/ft of treatment interval. A closed fracture acidizing stage with 28% HCl was pumped at the end of the treatment at a very low rate to increase the near wellbore etching and conductivity. Rahim et al.[3] noticed that even though the treatments were pumped in excess of 50 bpm, the loss of net pressure resulted in creating shorter fracture lengths. Therefore, today's treatments are designed with 3-4 stages of alternating pad and acid with acid volumes of 800 - 1,200 gals/ft. This re-design has significantly improved the success of sustaining positive net pressure during the treatment. Along with the multiple stages of pad and gelled acid, emulsified acid was also introduced in an attempt to obtain deeper penetration of the stimulation fluids.[3]

CHAPTER V

EVALUATION

This chapter includes a complete analysis for the first two cases, SA-1 and SA-2. For the other three cases I compare the fracture geometry which was obtained by the design model with value obtained by the equations related to the acid fracture number concept. This comparison will be discussed in the next section

5.1   Fracture Geometry and Dimensionless Parameter

The design model predicts some of the fracture geometry parameters such as fracture half length, x_f, dimensionless fracture conductivity, C_{fD}, effective conductivity, kw_{af} and fracture width, w. In order to compare the design parameter with the value obtained by the dimensionless group equations given by **Eq's.2.5** and **2.7**. One can calculate these parameters and compare both results. In my research work I compared the deign parameters as give by the fracCADE model (Approach 1) with the calculated parameters using **Eq's.2.5** and **2.7** (Approach 2). However in the two approaches the fracture half length assumed to be the design value.

5.1.1   Approach 1 (Fracture Geometry Parameters Obtained by fracCADE Model)

Approach 1 applies uses the fracture geometry that was predicted before the fracturing treatment using the design model (fracCADE) provided by the designing service company. In Approach 1, I used the fracture half length, average width, dimensionless fracture conductivity and effective conductivity from the model, FracCADE. However, I

calculated the acid fracture number using **Eq. 2.7**. After that, at a know value of ($C_{fD,}$ N_{af}), the dimensionless productivity index can be located in either **Figures 2.1** or **2.2**.

5.1.2 *Approach 2 (Fracture Geometry Parameters Obtained by Dimensionless Groups Equations)*

In Approach 2, I use the fracture half length only, and average width from the model design using fracCADE. After that, **Eqs.2.5** and **2.7** can be used to calculate the dimensionless fracture conductivity and the effective conductivity respectively. Similar to the first approach, I calculated the acid fracture number using **Eq. 2.7**. Then, at a known value of ($C_{fD,}$ N_{af}), the dimensionless productivity index can be located in either **Figures 2.1** or **2.2**.

In Approach 2, I calculated the fracture width by using the ideal width formula, **Eq. 2.10**. The only fracture geometry parameter needed from the design program output is the fracture half length.

Also, the acid volume is needed to calculate the ideal width. That can be estimated from the design treatment provided by the service company. Knowing the slurry volume and the acid amount that has been added in each stage, one can calculate and the exact amount of the acid that has been pumped. **Table 5.1** summarizes the volumes of acid pumped into well SA-1. For that particular well, the total acid volume was 81,801 gallon. Using the dissolving power of 28 wt% HCl, the calculated fracture width is 0.19 inch. Column 3 and Column 4 in **Table 5.2** represents the data obtained with Approach 1 and 2 respectively.

TABLE 5.1-PUMPING SCHEDULE FOR SA-1				
Stage Name	Slurry Rate (bbl/minute)	Pump Time (Minute)	Slurry Volume (bbl)	Acid Volume (gal)
Pad (polymer gel)/ Acid	48.5	9.3	451	16,879
Pad (polymer gel)/ Acid	58.4	7.4	432	16,172
Pad (VES)/ Acid	64.6	6.6	426	15,955
Pad (VES)/ Acid	67.4	8.9	599	22,447
Closed Fracture Acid	55.3	5	276	10,347

SA-1: The design model provide an estimate of the fracture length of 378 ft, a value of dimensionless fracture conductivity of 34, fracture conductivity of 26,413 md-ft, and an average fracture width of 0.16 inch. Those values represent the Approach 1. Applying Approach 2, both the effective conductivity and the dimensionless fracture conductivity calculated to be 28,729 md.ft and 31, respectively. Also, the fracture width was calculated to be 0.19 inch. **Table 5.2** shows a comparison between the model values and the calculated values using the two approaches. The deviation percent indicate that there is a discrepancy between those values range from 5 to 15%.Usign the "Acid Fracture Number" concept, the dimensionless productivity index can be estimated by knowing both acid fracture number, N_{Ac} and dimensionless fracture conductivity which was calculated to be 0.2 and 34.2 respectively. Based on the last two values, the dimensionless productivity index, J_D was estimated to be 0.37. This value reflects the performance of the well at the very early stage after putting the well on the production line following the acid fracturing treatment.

TABLE 5.2- SA-1 FRACTURE GEOMETRY AND DIMENSIONLESS PARAMETER				
Parameter	Symbol	Design Value	Calculated Value	Deviation %
Fracture Geometry				
Fracture half length, ft	x_f	378	378	---
Average width, in	w	0.16	0.19	15
Dimensionless fracture conductivity	C_{fD}	34	31	10
Effective conductivity, md-ft	kw_{af}	26,413	28,279	6
Results from Acid fracture Number Concept				
Acid fracture number	N_{af}	0.19	0.20	5
Dimensionless productivity Index	J_D	0.37	0.38	2

Similar analyses were done to SA-2, as shown in **Table 5.3**. The dimensionless productivity index obtained by the first two approaches turned out to be the same, which reflects the overall productivity index. **Appendix A** includes the fracture geometry and the dimensionless parameter for the other cases.

TABLE 5.3- SA-2 FRACTURE GEOMETRY AND DIMENSIONLESS PARAMETER				
Parameter	Symbol	Design Value	Calculated Value	Deviation %
Fracture Geometry				
Fracture half length, ft	x_f	413	413	---
Average width, in	w	0.21	0.16	30
Dimensionless fracture conductivity	C_{fD}	98.4	83.4	18
Effective conductivity, md-ft	kw_{af}	48,475	57,132	15
Results from Acid fracture Number Concept				
Acid fracture number	N_{af}	0.59	0.69	14
Dimensionless productivity index	J_D	0.38	0.39	2

The fracture width, which was calculated by the ideal width equation, has a value greater than the model value except, for SA-2, the deviation percent vary between 15 and 34%. **Figure 5.1** summarizes the fracture width with the deviation percent between the values obtained by Approach 1 and 2. Notice that Case 3 and 4 represent SA-3, K-B and SA-3, K-C respectively.
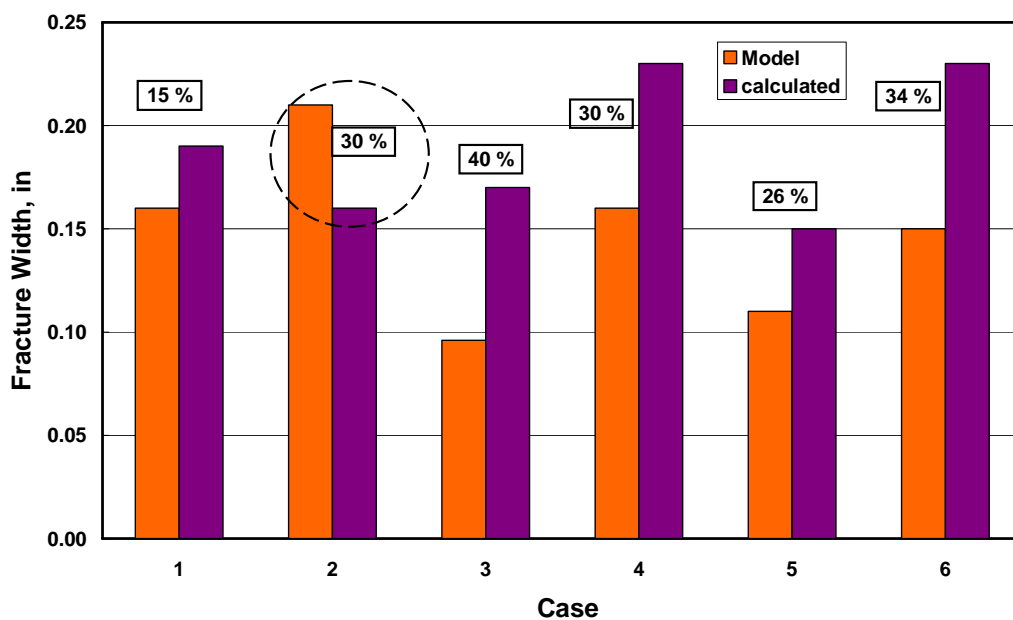
Fig. 5.1-Comparison between the calculated and the design fracture width for 6 acid fracture treatments. Where
1 = SA-1
2 = SA-2
3 = SA-3, K-B
4 = SA-3, K-C
5 = SA-4
6 = SA-5

5.2   Bottomhole Pressure Calculation

In this study, production data were available for only two of the wells, SA-1 and SA-2. The flowing bottomhole pressure (FBHP) was calculated using the inflow performance relationship (IPR) and the vertical lift performance (VLP). Because the procedure must

be done for more than 40 data point, it can be time consuming to do by hand. To computerize the process. I used the nodal analysis model PERFORM[27] to compute values for the FBHP model can be used

Well PERFORMance Analysis (PERFORM) is a graphical tool which can be used to analyze the performance of an oil or gas well. PERFORM can analyze multi-layer and /or multilateral reservoirs. Both production and injection wells can be modeled with both empirical and mechanistic pressure drop correlations. The model can be used friendly to calculate the inflow and outflow curves for a given well, using different nodes: bottomhole, wellhead and separator for onshore wells and bottomhole, top of tubing, riser outlet and flow-line outlet for offshore wells. In my study I used the FBHP (bottomhole flowing pressure) as a node.

The data required by the model to perform the calculation for each FBHP are listed in **Table 5.4** for SA-1.

TABLE 5.4- DATA INPUT TO CALCULATE THE FBHP USING PERFORM		
Input	**Value**	**Unit**
Condensate Gravity	46.2	^oAIP
Specific Gas Gravity	0.79	---
Inorganic Content	$CO_2 = 1.53$ $H_2S = 0.9$ $N_2 = 8.5$	%
Reservoir Temperature	270	^oF
Reservoir Permeability	2.22	md
Reservoir Thickness	151	ft
Wellbore Radius	3.5	inch
Reservoir Radius	5553	ft
Casing / Tubing Diameter	6.094' and 4.778'	inch
Reservoir Pressure	7436	psi
Reservoir Skin	- 6.92	---
Wellhead Pressure	4788	psig
Output		
Bottomhole Flowing Pressure	6410	psi

In **Table 5.3** the last three input are the only values to change to calculate the FBHP at the end of each month in a specific well. These values include flowing wellhead pressure (FWHP), average reservoir pressure, and productivity index represented by skin factor.

After entering the data in **Table 5.4** in the simulation model, an example of the output results which include the calculated FBHP is shown in **Figure 5.2**. This data point is the calculated FBHP in SA-1 @ (2nd Month of production, FWHP = 4,788 psig, average reservoir pressure = 7,436 psig and skin = -6.93).
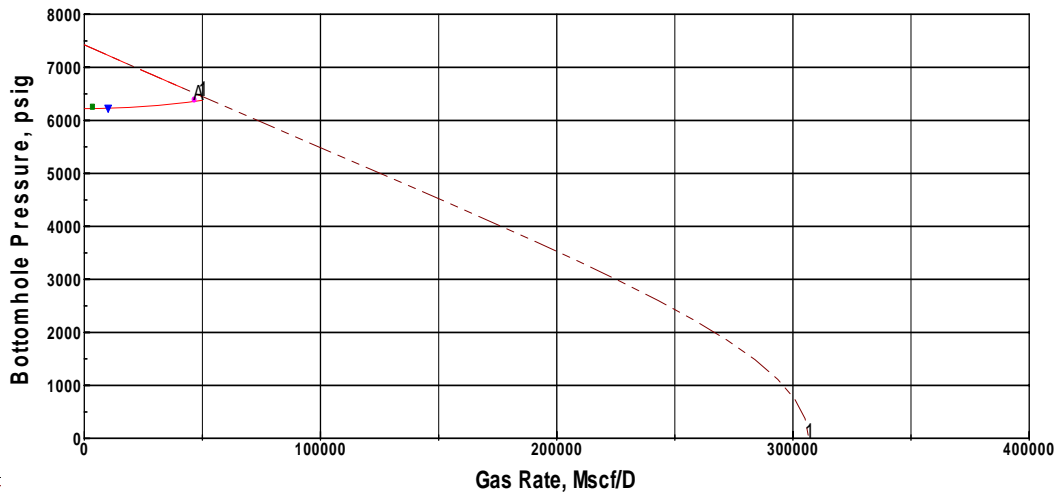
Fig. 5.2-Example of FBHP calculation using PERFORM, the plot represents a combination of inflow performance relationship (IPR) and vertical lift performance (VLP).

The same procedure can be repeated for each FWHP, and the FBHP can be calculated. **Table B.1** and **B.2** in **Appendix B** includes a set for the data needed by the model to calculate the FBHP for 25 month period of time with the output results for SA-1 and SA-2 respectively.

<u>SA-1:</u> **Figure 5.3** shows the change in the FBHP as the well being produced for long time. In this case the production data were available for more than two years. For the first 18 months, the FBHP decreased slightly from 6,442 to 5,839 psi. After that, there was a sharp drop in the FBHP along the following three months 19th, 20th, and 21st. Then the pressure level to about 4,500 psi. The cause of this decline will be discussed in the next chapter. The corresponding change in the reservoir pressure as shown in **Figure 5.3** described by gradual decrease from initial value of 7,500 to 6,806 psi with 10% reduction in the potential pressure of the reservoir. During the production interval the

choke valve has a back pressure between 1,270 and 1,622 psi with an average value of 1,478 psi.
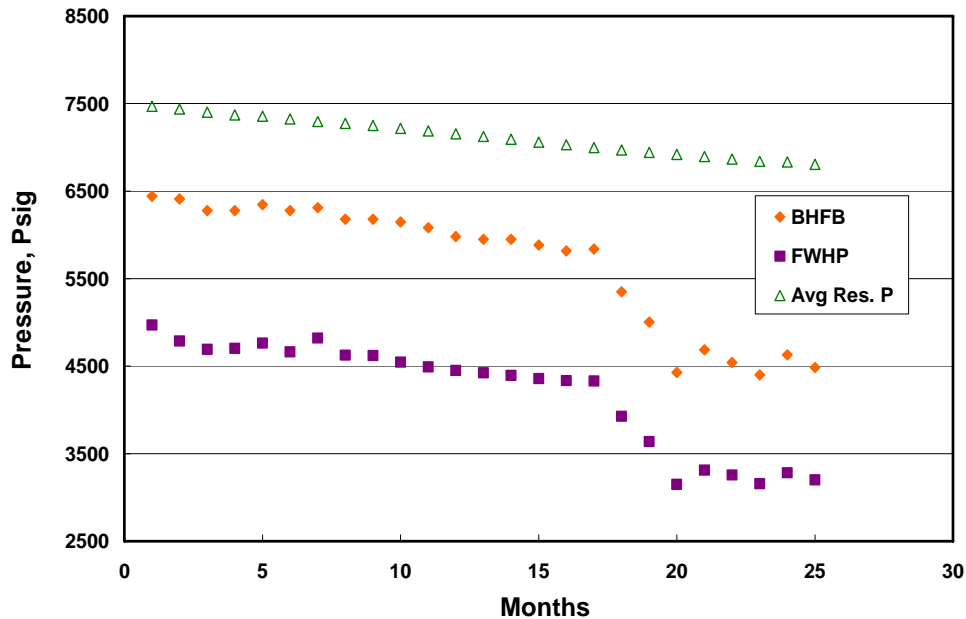
Fig. 5.3-The change in the reservoir pressure, FBHP and FWHP with time for SA-1.

SA-2: In this case the behavior of the FBHP was fluctuating over a period of time as shown in **Figure 5.4**. At the beginning of the production time the FBHP estimated to be 5,752 psi. However, the FBHP decline in Sinusoidal shape. The lowest pressure occurs at about 5,000 psi.   Many reasons can explain such instability as it will be discussed later. **Appendix B** includes a tabulated data for the different pressure values.
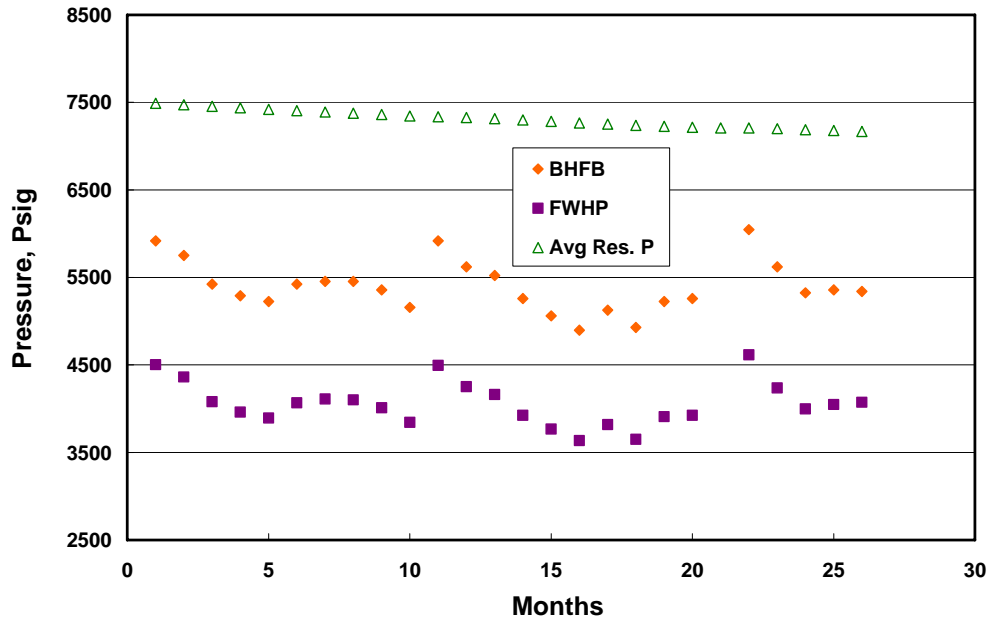
Fig. 5.4-The change in the reservoir pressure, FBHP and FWHP with time for SA-2.

5.3   Effective Fracture Conductivity

To calculate the fracture conductivity, I used Nierode-Kruk[14] Correlation. Two important parameters affect the result significantly. First, rock embedment strength is very important. Second, the net closure stress acting on the fracture faces which is the difference between the in-situ stress and the FBHP. Based on literature review[15] and personal communications, 100,000 psi chosen to be the embedment rock stress for such formation.

Figure 5.5 shows the calculated fracture conductivity against the change in the FBHP which is related directly to the closure pressure. Clearly, the higher FBHP the better conductivity as it will act against the minimum in-situ stress.

In case SA-1 the calculated fracture conductivity at the first month of production was 28,600 md-ft. This value was very close to the design value which was reported as

28,700 md-ft. According to Nierode-Kruk correlation the corresponding fracture conductivity to the decline in FBHP shows a sever reduction in the first one. The conductivity decreases from 28,606 md-ft to 9,259 md-ft. This number may not reflect the exact picture but still it shows how the fracture conductivity change as the closure stress increases.

However, in SA-2 the design value was 7 times grater than the calculated value which was reported as 57,132 md-ft. This difference suggested that, the design value was over estimated in some cases.
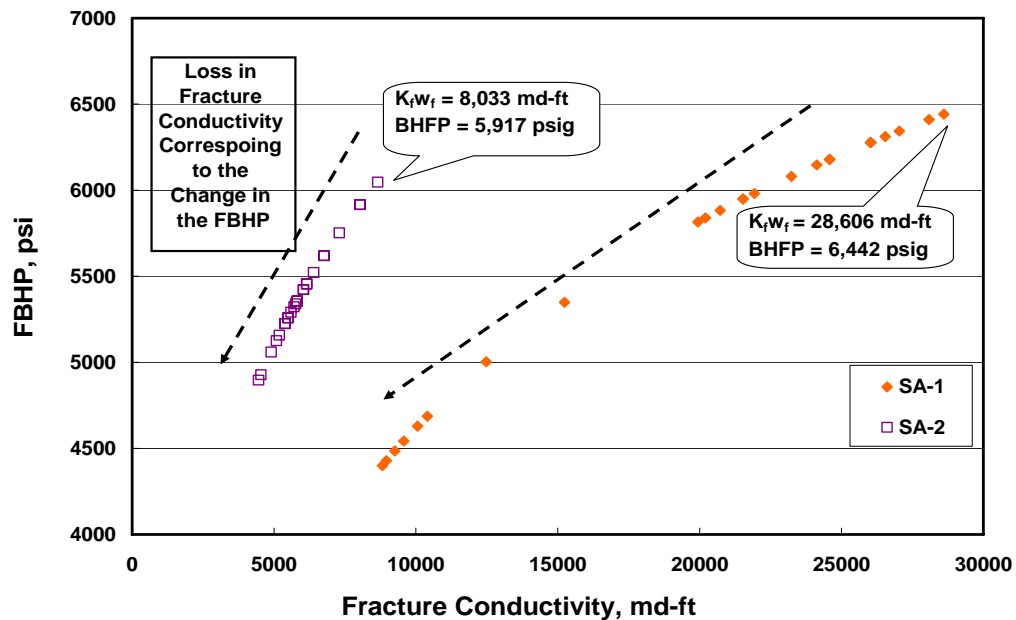
Fig. 5.5-The change in fracture conductivity as the FBHP decline with time.

5.4   Productivity Index Analysis

One of the main analysis to describe the performance of the well is to calculate the productivity index. This can be done by solving **Eqs. 2.11** through **2.14**. The

productivity index for SA-1 given in **Figure 5.6** indicates instability in the production at the first few months after the production. This was confirmed later as a result of transition to pseudo-steady state from infinite acting behavior which takes between 3 and 6 months. **Eq. 2.15** was used to calculate this time. After that the well continues producing until a sudden drop in the productivity index. In case of SA-1 the drop resulted in more than 40% reduction in the PI.
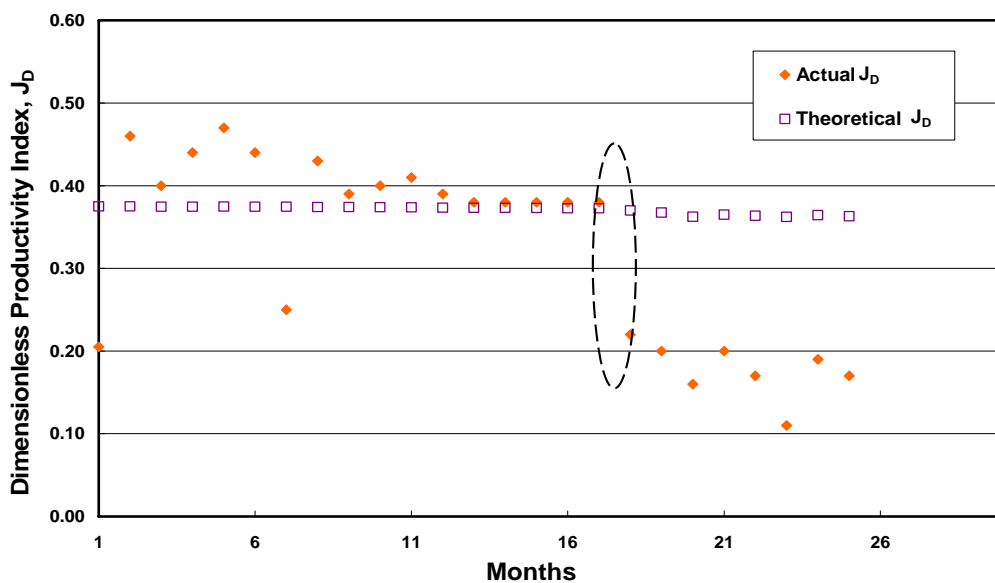
Fig. 5.6-The change in the productivity of the well with time for SA-1.

In SA-2 the productivity index decreases from 0.27 to 0.15 as shown in **Figure 5.7**. However, the trend shows the productivity index declines in three stages. At the beginning of each stage it looks like if the well is picking up some of the productivity but soon it declines again.
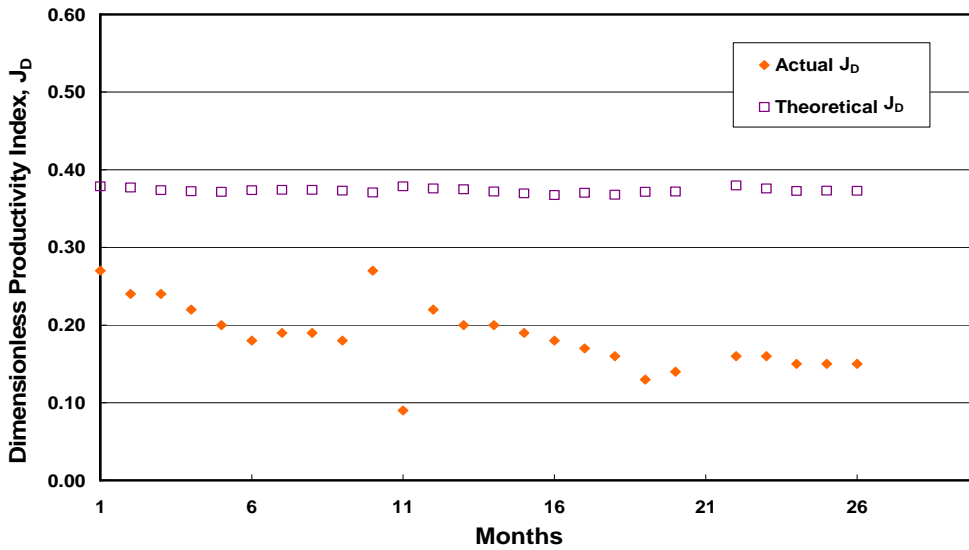
Fig. 5.7-The change in the productivity of the well with time for SA-2

To show the behavior of the productivity index if 50,000 psi chosen to be the rock embedment strength, similar analysis were done to calculate the productivity index using rock embedment strength of 50,000 psi as shown in Figure **Figs. 5.8** and **Figs. 5.9** for SA-1 and SA-2, respectively.
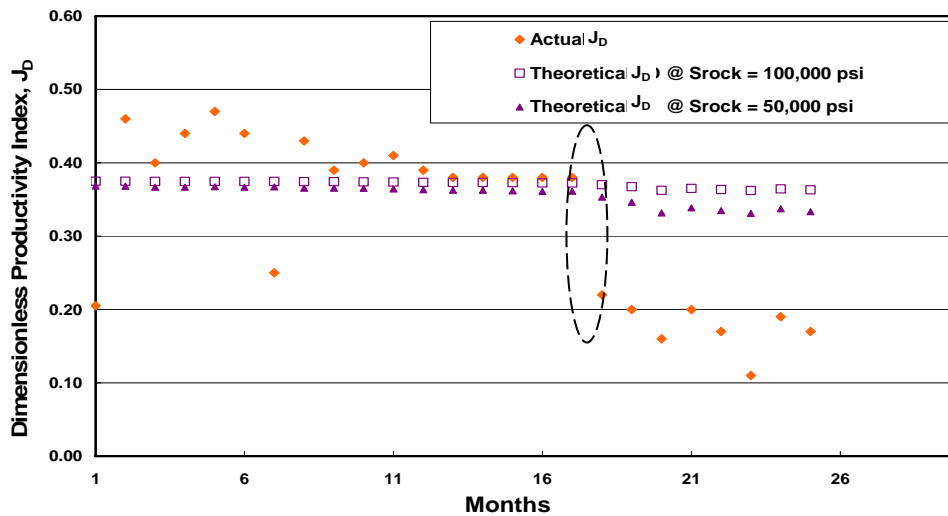
Fig. 5.8-The change in the productivity of the well with time for SA-1 @ S_{rock} = 100,000 and 50,000 psi.
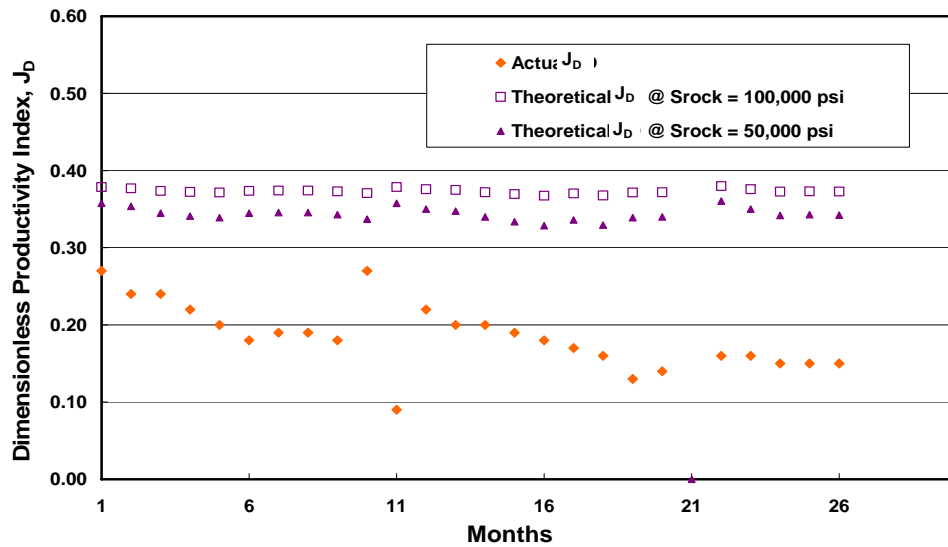
Fig. 5.9-The change in the productivity of the well with time for SA-2 @ S$_{rock}$ = 100,000 and 50,000 psi.

The estimated dimensionless fracture conductivity for SA-1 after the acid fracturing treatment decreases from 34 to 10 at constant J$_D$ of 0.37 as **Figure 5.10** shows. This suggested that the well was over-fractured in terms of width. Similar thing happens in SA-2, the dimensionless fracture conductivity lowered from 14 to 10.
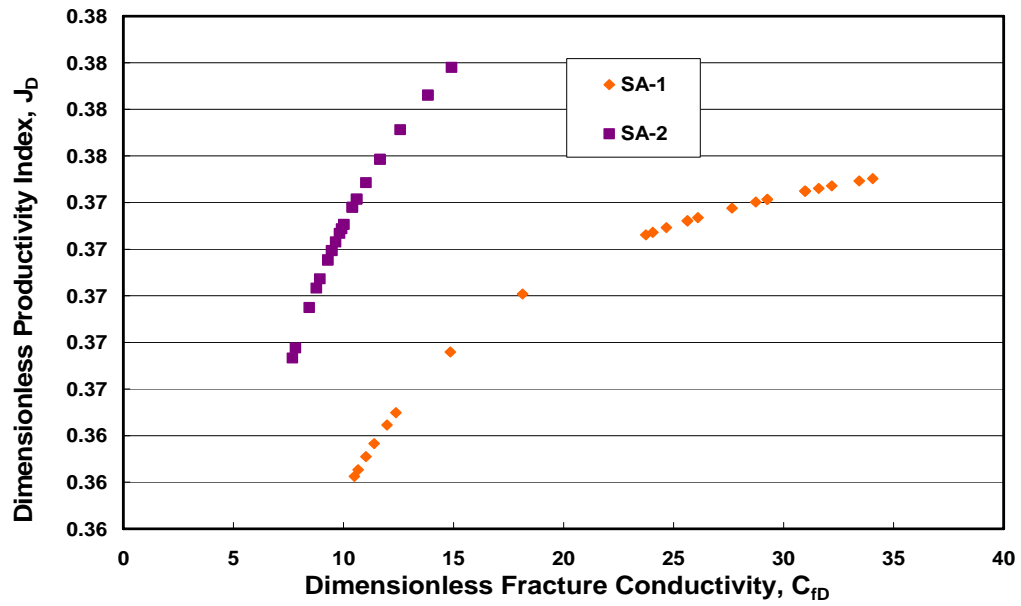
Fig. 5.10-The change in the J$_D$ verses the dimensionless fracture conductivity.

Appendix B includes a list for the dimensionless group for SA-1 and SA-2.

CHAPTER VI

DISCUSSIONS

From **Chapter V**, it was clear that the PI changes over time. In this chapter, I will discuss several possible reasons which can cause such variation. These include:

- Liquid dropout as pressure reaches dew point.

- Net closure pressure effects on fracture conductivity.

- Non-Darcy effects on overall productivity.

- Pressure and in-situ stress effects on reservoir permeability.

I will focus on the first three items. However, the possible detritions of reservoir permeability is not included in this study.

6.1   Possible Reasons for the Change in the Productivity Index Behavior

6.1.1   Condensate Dropout

The fundamental mechanism in a gas condensate system can be describe as the rich gas approaches the wellbore, the pressure drops below the dew point causing liquid hydrocarbons to condense in the reservoir. Due to relative permeability effects, the effective permeability to gas is reduced, which decreases well deliverability. **Figure 6.1** shows how the condensate forms in the pore throat of the rock formation
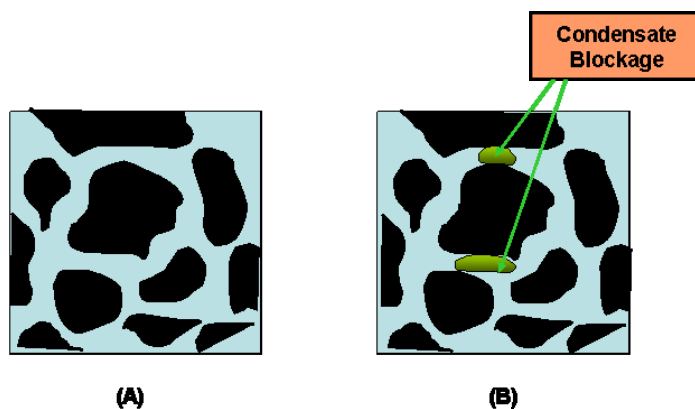
Fig. 6.1-The accumulation of gas condensate in the pore-throat. (A) Pore-throat before condensate; (B) After condensate.

In order to plot the phase envelop, an accurate PVT data are needed for the gas composition. **Table 6.1** summarizes the component that represents the gas composition of SA-1. To validate the data, I did a flash point calculation and compare the PVTsim[28] results with the lab results as shown in **Table 6.2**.

TABLE 6.1-GAS COMPOSITION FOR SA-1	
Component	**Well Stream Mole%**
Nitrogen	7.6
Carbon Dioxide	0.93
Hydrogen Sulfide	0.00
Methane	72.61
Ethan	7.79
Propane	3.45
i - Butane	0.63
n - Butane	1.30
i - Pentane	0.44
n - Pentane	0.49
Hexanes	0.59
Heptanes	0.73
Octanes	0.74
Nonanes	0.61
Decanes Plus	2.09
Total	**100.00**

TABLE 6.2-FLASH POINT CALCULATION FOR SA-1				
	LAB Results		PVTsim[28]	
Component	Sep. Liquid Mole%	Sep. Gas Mole%	Sep. Liquid Mole%	Sep. Gas Mole%
Nitrogen	0.89	8.2	1.02	8.14
Carbon Dioxide	0.32	0.98	0.50	0.96
Hydrogen Sulfide	0.00	0.00	0.00	0.00
Methane	22.26	77.11	21.96	76.83
Ethan	6.21	7.93	6.65	3.247.88
Propane	5.58	3.26	5.91	3.24
i - Butane	1.58	0.54	1.67	.54
n - Butane	4.1	1.05	4.14	1.06
i - Pentane	2.24	0.28	2.07	0.30
n - Pentane	2.87	0.28	2.56	0.31
Hexanes	5.08	0.19	4.39	0.27
Heptanes	7.79	0.10	7.17	0.19
Octanes	8.62	0.04	8.05	0.13
Nonanes	6.96	0.04	7.16	0.06
Decanes Plus	25.5	0.00	26.68	0.04

Using the gas composition for SA-1, I was able to draw the phase envelop using the PVTsim[28]. **Figure 6.2** shows the phase envelop for SA-1. From the graph it is clear to observe the dew point at 270°F as 5,650 psi. Therefore, any pressure in or around the wellbore fracture below 5,650 psi can result in condensate dropout and accumulation. Recall **Figure 5.3,** the decrease started after the 18th month at BHFP of 5,349 psi. This support the suggestion that the sudden decrease in the PI is dominated by the condensate blockage.
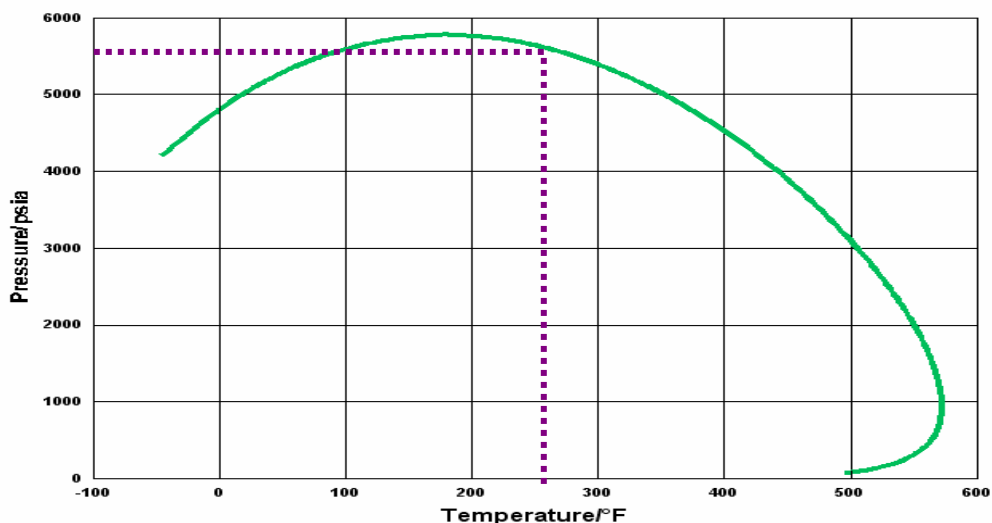
Fig. 6.2-Phase envelope diagram generated by PVTsim at a given gas composition.

Based on simulation studies Rahim *et al.*[29] reported that the near wellbore condensate saturation can quickly reach over 30% within 200-300 ft of radius.

Carlson *et al.*[30] investigate the effects of retrograde liquid condensation on a well productivity for a fracture well. In his paper, Carlson found that for a well containing a hydraulic fracture, the deliverability did not seem to be strongly affected by liquid drop out. These results appeared to contradict the other work done by other scientists such Fussell[31] and the reason for that because in their work they had used an equivalent wellbore radius to account for the fracture effect. This approach apply the assumption of radial flow around the wellbore which imply significant reduction in the well deliverability is a result of condensate drop out. If this applied to the case I investigated, it support the suggestion that the reduction in the well I investigated was a result of sever reduction in the conductivity which makes the flow around the wellbore as radial flow and the condensate dropout is the real cause for such reduction.

In the second case, the productivity index did not show a sharp decline as SA-1. Since I do not have the gas composition it will be difficult to determine the dew point where the liquid comes out of the solution. However, since both well located in the same area and produce from similar zone, which means the phase envelop is going to be very similar. **Figure 6.2** shows that the dew point occurs at about 5,750 psi when reservoir temperature set at 250 ^{o}F. Going back to **Figure 5.4**, the well start producing at FBHP calculated to be 5,752 psi. Clearly this pressure is already at dew point which means the condensate blockage is acting. An important notice is that the slight decline in the production followed by stable or increase in some cases. This pattern was explained by El-Banbi[32]. He noted that the productivity inclines of the wells in a moderately rich gas condensate reservoir were observed to initially decrease rapidly, and then increase as the reservoir was depleted as explained by El-Banbi,

"During early production, a ring of condensate rapidly formed around each wellbore when the near-wellbore pressures decreased below the dew point pressure of the reservoir gas. The saturation of condensate in this ring was considerably higher than the maximum condensate predicted by the PVT laboratory work due to relative permeability effects. This high condensate saturation in the ring severely reduced the effective permeability to gas, thereby reducing gas productivity. After pressure throughout the reservoir decreased below the dew point condensate formed throughout the reservoir, thus the gas flowing into the ring became leaner causing the condensate saturation in the ring to decrease. This increased the effective permeability of the gas. This caused the gas productivity to increase as was observed in the field."

There are many ways to reduce the effect of gas condensate around wellbore area. One way is to inject lean gas (Cvetkovic et al., 1990).[33]Another way is to inject nitrogen (Sanger and Hagoort, 1998).[34] Many reasons limit the implementation of any of the previous methods either for economic reasons or for technical difficulties.

The producing rate of gas condensate reservoirs is affected greatly by the flowing bottomhole pressure. The value of the bottomhole pressure controls the amount and distribution of liquid condensate. Obviously, one way to prevent the formation of condensate is to maintain the FBHP to be above the dew point pressure. From practical point of view this is not possible since average reservoir pressure will drop as cumulative production reaches sensible values.

6.1.2   *Changing Fracture Conductivity*

There are two factors controlling the stability of the fracture conductivity. These two factors are the net closure pressure and the rock embedment strength. **Figure 6.3** shows how the fracture conductivity responds to the change in the embedment rock strength and the net closure pressure. The middle line belongs to SA-1 as the embedment strength change from 20,000 to 120,000 psi. Noticed that the value at rock embedment strength of 100,000 psi and closure stress of 4000 psi is the fracture conductivity of SA-1 which was estimate to be 28,600 md-ft after the acid fracturing treatment.
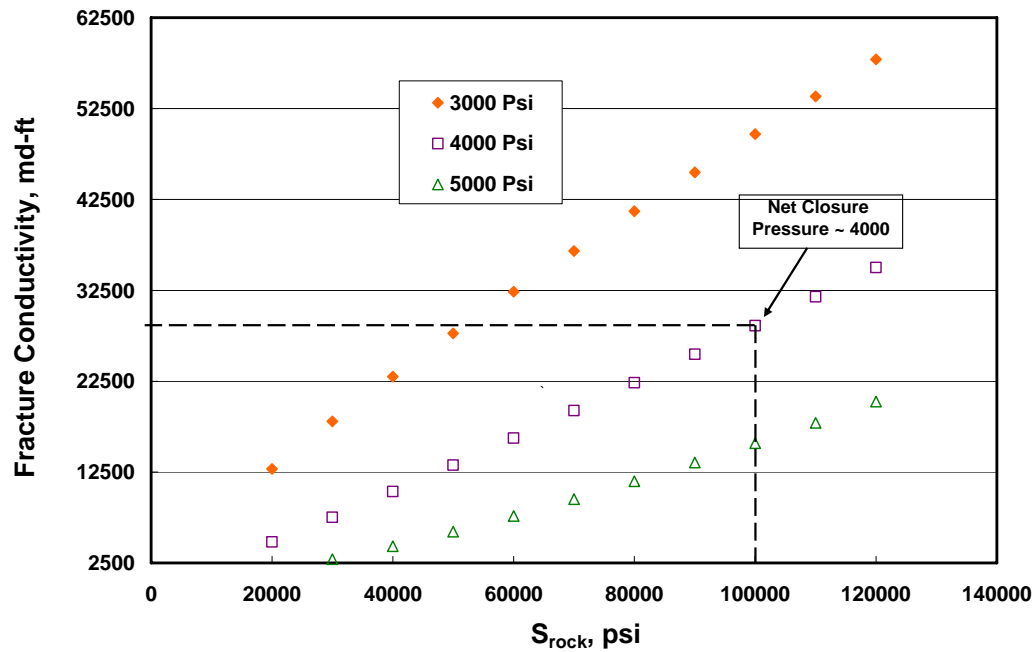
Fig. 6.3-The effect of embedment stress on the fracture conductivity at different net closure pressure.

As shown in **Figure 6.3**, Reducing the closure pressure in SA-1 at the early stage by 1,000 psi increase the fracture conductivity from 28,600 md-ft to 50,000 nd-ft.

6.1.3   Other Possible Reasons

Non-Darcy flow and changing permeability is another possibility for such decline. In the next section I will discuss the non-Darcy flow effect. However, the changing in the permeability is not covered in this study.

Non-Darcy flow is a result of any turbulence effect in the flow bath. In gas well, condensate can increase the turbulence as a result of introducing another phase to the system. The non-Darcy effect has more influence on the production decline as the rate increase. In Fracture well, this phenomena can be eliminated if a long fracture were

created to flow the gas from the reservoir to the wellbore. Since all the cases I tested have a fracture half length more than 300 ft, this length neglects the turbulence effects.

Rahim *et al.*[29] analyzed multi-rate test for similar cases. His observation was that all of the wells had build-ups following the last rate and none of the wells exhibited any turbulence effects during any of the flow or build-up periods of the test. As a result, turbulence can be neglected.

Gidley *et al.*[35] reported that a dimensionless fracture conductivity of 10 typically is assumed to provide a fracture so permeable in a way that formation permeability, not fracture permeability, controls the flow resistance. He mentioned that unless fracture conductivity is corrected for non-Darcy flow effects, this can cause a serious deficiency in fracture conductivity which will indicate less production than the expected one for the fracturing treatment. Gidley, Concluded that the dimensionless fracture conductivity can be corrected for non-Darcy flow be dividing it by the term $(1+N_{RE})$.

We found that non-Darcy flow can not explain the apparent change in productivity at later time because its effect should rather decrease with production decline.

6.2   Proppant Fracture as an Alternative

In both wells, the acid fracture number ranged from 0.1 to 0.2. In a medium permeability this can be the optimum scenario. However, since we are dealing with low permeability formation, massive hydraulic fracture is another option to consider resulting in J_D ranged between 1 and 1.5 as shown in **Figure 6.4**. To obtain this J_D, massive proppant fracturing treatment with larger acid fracture number in needed.

There are two reasons why proppant fracturing is recommended in this case. First, it will result in longer fracture. Second, proppant fracture is more reliable when maintaining conductivity becomes a concern.
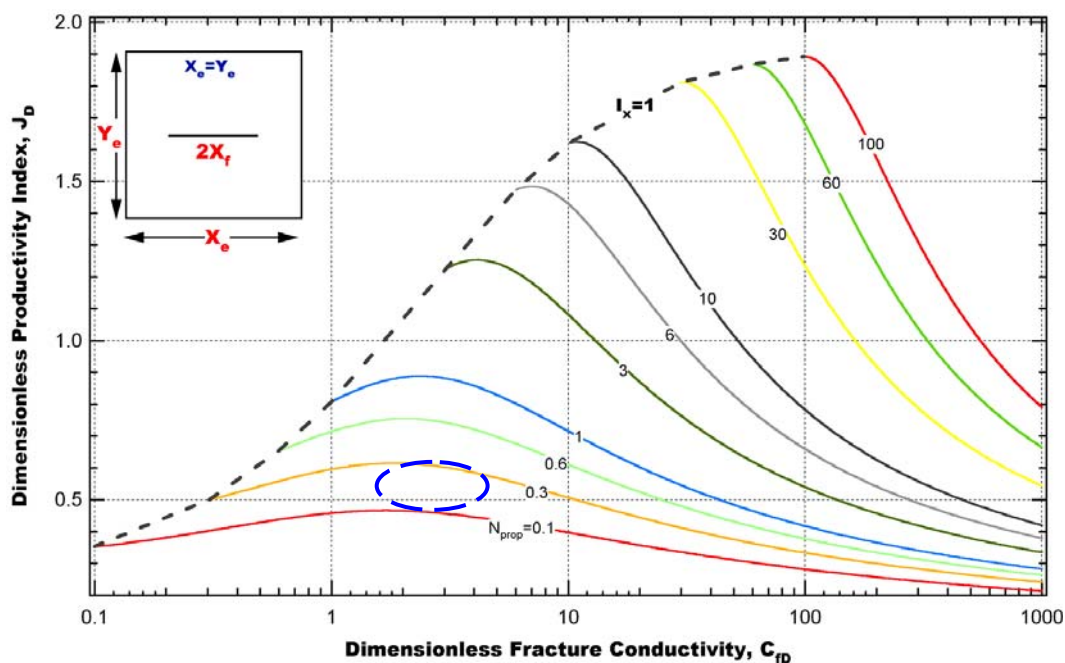
Fig. 6.4- Fracture performance as a function of dimensionless fracture conductivity for medium\high acid number. Reproduced from SPE paper 73758.[18]

Proppant fracturing can create longer fractures and has potential for application in such fields. Proppant fracturing of carbonate reservoirs is getting more attention in the industry.[36,37,38] In proppant fracturing, a propping agent is used to keep the fracture open for the life of the well. Longer fracture half-lengths and sustainable conductivity are the leading drivers for this technology. However, for low-permeability reservoirs, longer fracture half length proved to be a main goal in such treatment. On the other hand, in high permeability reservoirs, fracture width is a key parameter to create better conductivity.

Wang *et al.*[39] showed that the production from gas condensate reservoirs should be a result of an optimization of distribution of the liquid condensate around the fracture. Two main fracture geometries should be design for an optimal value, the fracture half length and the fracture width. An important parameter to consider is the permeability.

The important of permeability comes from the fact that fracture face damage can be sever as a result of the penetration of polymer damage. In high-permeability cases this can significantly affect the production in. Whereas, the impact is less significant in low permeability. In the given study cases the permeability considered to be low and ranged from 0.5 to 4 md. Also, the fracture fluid was viscoelastic surfactant, the fluid prove to be a non-damage fluid and had a high efficiency to recover.[8]

CHAPTER VII

CONCLUSIONS AND RECOMMENDATIONS

7.1   Conclusions

On the basis of my research, we offer the following conclusions:

1. The fracturing model tend to overestimate the fracture conductivity in some cases as shown in SA-2

2. Production behavior response of all wells exhibits instability in the production for the first 3 to 6 months, which is the transition time to pseudo-steady state from infinite acting behavior and when the hydraulic fracture is closing.

3. The calculated fracturing width using the ideal width equation was 30% more than the design value.

4. Both near-well liquid drop-out and fracture-conductivity deterioration can impact the production in different proportion.

5. A possible reason for the sharp decrease in the productivity index is the liquid dropout.

6. Non-Darcy flow initially can not explain apparent change in productivity since its effect should decline with production decline.

7.   The "Acid fracture Number" concept proves to be an effective way to evaluate the acid fracturing treatment.

7.2   Recommendations

Based on my research work, several recommendations were made as the following:

1. Better fracture conductivity leads to less draw down and maintains the flowing bottomhole pressure above the dew point.

2. Better design can be achieve with using the commercial fracturing model if integrated with "Acid Fracture Number" concept

3. It is necessary to know the condition of the well if already reach the dew point prior the acid fracturing.

4. It is recommended to measure the GOR to make better judgment about the condensate possibility.

5. The study cases have an acid fracture number ranged between 0.1 and 0.2. with this acid number the maximum productivity we can get is 0.6 Theoretically, since we have tide formation, a better hydraulic fracture should give productivity index range from 1.0 to 1.5 based on the acid fracturing number.

6. Proppant fracturing can help in maintaining the well performance for longer time if applied for optimal design.

NOMENCLATURE

A Reservoir area, acre

B Formation volume factor (resbbl/STB)

B_{gi} Initial gas formation volume factor (resbbl/STB)

C_t Total fluid loss coefficient

C_{fD} Dimensionless fracture conductivity

D Pipe diameter, inch

G_i Initial gas in place, SCF

f_f Friction factor

h Net thickness, ft

h_p Net Pay thickness, ft

I_x Penetration ratio, x_f/x_e

k Reservoir permeability (horizontal if not denoted), md

kw_{af} Effective conductivity, md-ft

L Length of vertical line, ft

N_{af} Acid fracture number

$\bar{p}$ Average reservoir pressure, psi

p_{avg} Average reservoir pressure, psi

p_{wf} Flowing bottomhole pressure, psi

p_1 Upstream pressure, psi

p_2 Wellhead pressure, psi

q Gas flow rate, MSCF/d

r_e Equivalent drainage radius, ft, m

r_w Wellbore radius, ft, m

S_{rock} Rock embedment stress, psi

S_g Gas saturation, %

T Temperature, °R

T_{pss} Pseudo-steady state, hr

V Injected acid volume, bbl

w Fracture width, in

w_i Ideal width, in

x_e Equivalent drainage length, ft

x_f Fracture half-length, ft

X Volumetric dissolving power

Z Gas deviation factor

Z_i initial gas deviation factor

μ Viscosity, cp

α_l Constant for appropriate units (141.2 for oilfield)

σ Net closure stress, psi

$\emptyset$ Porosity

Δp Net pressure in the fracture, psi

θ Deviation from vertical , Degree

γ_g Gas specific gravity

REFERENCES

1. Al-Qahtani, M.Y, and Rahim, Z.M.: "A Mathematical Algorithm for Modeling Geomechanical Rock Properties of the Khuff and Pre-Khuff Reservoir in Ghawar Field," paper SPE 68194 presented at the 2001 SPE Middle East Oil Show, Bahrain, 17-20 March.

2. Rahim, Z.M., and Patrick, M.: "Sustained Gas Production from Acid Fracture Treatment in the Khuff Carbonates, Saudi Arabia: Will proppant Fracturing Make Rates Better? Field Example and Analysis," paper SPE 90902 presented at the 2004 SPE Annual Technical Conference and Exhibition, Houston, Texas, 26-29 September.

3. Rahim, Z.M., Bartko, K.M., and Al-Qahtani, M.Y.: "Hydraulic Fracturing Case Histories in Carbonate and Sandstone Reservoirs of Kuff and Pre-Kuff Formations, Ghawar Field, Saudi Arabia," paper SPE 77677 presented at the 2002 SPE Annual Technical Conference and Exhibition, San Antonio, Texas, 29 September- 2 October.

4. Al-Qassab, H.M., Al-Khalifa, M.A., Al-Ali, Z., Ameen, M., and Phillips, R., *et al*.: "New Integrated 3D-Fracture Modeling and Flow Simulation Study: A Giant Saudi Arabian Carbonate Reservoir," paper SPE 78295 presented at the 2002 SPE 13th European Petroleum Conference, Aberdeen, Scotland, 29-31 October.

5. Nasr-El-Din, H.A., Al-Driweesh, S., Al-Muntasheri, G.A., Marcinew, R., and Daniels, J., *et al*.: "Acid Fracturing HT/HP Gas Wells Using a Novel Surfactant Based Fluid System," paper SPE 84516 presented at the 2003 SPE Annual Technical Conference and Exhibition, Denver, Colorado, 5-8 October.

6. Rahim, Z.M., and Al-Qahtani, M.Y.: "Sensitivity Study on Geomechanical Properties to Determine Their Impact on Fracture Dimensions and Gas Production in the Khuff and Pre-Khuff Formations Using a Layered Reservoir System Approach,

Ghawar Reservoir, Saudi Arabia," paper SPE 72142 presented at the 2001 SPE Asia Pacific Improved Oil Recovery Conference, Malaysia, 8-9 October.

7. Rahim, Z.M., and Al-Qahtani, M.Y.: "Selecting Perforation Intervals and Stimulation Technique in the Khuff Reservoir for Improved and Economic Gas Recovery," paper SPE 68216 presented at the 2001 SPE Middle East Oil Show, Bahrain, 17-20 March.

8. Nasr-El-Din, H.A., Samuel, E., and Samuel, M.: "Application of a New Class of Surfactants in Stimulation Treatments," paper SPE 84898 presented at the 2003 SPE International Improved Oil Recovery Conference, Malaysia, 20-21 October.

9. Williams, B.B., and Nierode, D.E.: "Design of Acid Fracturing Treatments," *SPEJ* (July 1972) 849.

10. *Reservoir Stimulation,* K. Elsa (ed.), John Wiley & Sons. Ltd., England (2000).

11. Al-Muhareb, M.A., Nasr-El-Din, H.A., Samuel, E., Marcinew, R., and Samuel, M., *et al*.: "Acid Fracturing of Power Water Injectors: A New Field Application Using Polymer-Free Fluid," paper SPE 82210 presented at the 2003 SPE European Formation Damage Conference, Hague, The Netherlands, 13-14 May.

12. Nasr-El-Din, H.A., Tibbles, R., and Samuel, M.: "Lessons Learned from Using Viscoelastic Surfactants in Well Stimulation," paper SPE 90383 presented at the 2004 SPE Annual Technical Conference, Houston, Texas, 26-29 October.

13. Al-Ghamdi, A.H., Nasr-El-Din, H.A., Al-Qahtani, A.A., and Samuel, M.: "Impact of Acid Additives on the Rheological Properties of Viscoelastic Surfactants and Their Influence on Field Application," paper SPE 89418 presented at the 2004 SPE/DOE Fourteenth Symposium on Improved Oil, Tulsa, Oklahoma, 17-21 April.

14. Nierode, D.E., and Kruuk, K.F.: "An Evaluation of Acid Fluid Loss Additives, Retarded Acids, and Acidized Fracture Conductivity," paper SPE 4549 presented at

the 1973 SPE 48th Annual Fall Meeting, Las Vegas, Nevada, 30 September- 3 October.

15. Nasr-El-Din, H.A., Al-Mutairi, S.H., Al-Malki, M., Metcalf, S., and Wallace, W.: "Stimulation of a Deep Sour Gas Reservoir Using Gelled Acid," paper SPE 75501 presented at the 2002 SPE Gas Technology Symposium, Calgary, Canada, 30 April- 2 May.

16. Economides, M., Oilgeny, R., and Valko, P., *Unified Fracture Design*, Orsa Press, Alvin, Texas (2002).

17. Valkó, P.P. and Economides, M.J.: "Heavy Crude Production from Shallow Formations: Long Horizontal Wells Versus Horizontal Fractures," paper SPE 50421 presented at the 1998 SPE International Conference on Horizontal Well Technology, Calgary, 1-4 November.

18. Romero, D.J., Valkó, P.P., and Economides M.J.: "The Optimization of the Productivity Index and the Fracture Geometry of a Stimulated Well with Fracture Face and Choke Skins," paper SPE 73758 presented at the 2002 SPE International Symposium and Exhibition on Formation Damage Control, Lafayette, Louisiana, 20- 21 February.

19. Economides, M., Hill, A.D., and Economides, C.E., *Petroleum Production System*, G. Trentacoste (ed.), Prentice Hall Inc., Upper Saddle River, New Jersey (1993).

20. Gong, M., Lacote, S., and Hill, A.D.: "A New Model of Acid Fracture Conductivity Based on Deformation of Surface Asperities," paper SPE 39431 presented at the 1998 SPE International Symposium on Formation Damage Control, Lafayette, Louisiana, 18-19 February.

21. Navarrete, R.C., Miller, M.J., and Gordon, J.E.: "Laboratory and Theoretical Studies for Acid Fracture Stimulation Optimization," paper SPE 39776 presented at the 1998 SPE Permian Oil and Gas Recovery Conference, Midland, Texas, 23-26 March.

22. Rahim, Z. and Al-Qahtani, M. Y.: "Using Radioactive Tracer Log, Production Tests, Fracture Pressure Match, and Pressure Transient Analysis to Accurately Predict Fracture Geometry in Jauf Reservoir, Saudi Arabia," paper SPE 71650 presented at the 2001 SPE Annual Technical Conference and Exhibition, New Orleans, Louisiana, 30 September- 3 October.

23. Cleary, M.P.: "Critical Issues in Hydraulic Fracturing of High-Permeability," paper SPE 27618 presented at the 1994 SPE European Production Operations Conference and Exhibition, Aberdeen, Scotland, 15-17 March.

24. Robinson, B.M., Diyashev, I.R, Rahim, Z.M., Wolhart, S.L., and Salehi, I.A.: "Fracture Fluid Damage to High-Permeability Gas Reservoirs: It Can Make Difference," paper SPE 63106 presented at the 2000 SPE Annual Technical Conference and Exhibition, Dallas, Texas, 1-4 October.

25. Burgos, G., Buijse, M., Fonseca, E., Milne, A., and Brady, M., *et al.*: "Acid Fracturing in Lake Maracaibo: How Continuous Improvement Kept on Raising the Expectation," paper SPE 96531 presented at the 2005 SPE Annual Technical Conference, Dallas, Texas, 9-12 October.

26. Al-Qahtani, M.Y, and Rahim, Z.M.: "Optimization of Acid Fracturing Program in the Khuff Gas Condensate Reservoir of South Ghawar Field Saudi Arabia by Managing Uncertainties Using State-of- Art Technology," paper SPE 71688 presented at the 2001 SPE Annual Technical Conference and Exhibition, New Orleans, Louisiana, 30 September- 3 October.

27. *PERFORM Software*, Version 5.00, HIS ENERGY, Dallas, Texas, (2004).

28. *PVTsim Software*, Version 14, Calsep, Houston, Texas, (2004).

29. Rahim, Z.M., and Ahmed, M.: "Analysis of Long-Term Production Performance in Acid Fractured Carbonate Wells," paper SPE 95988 presented at the 2005 SPE Annual Technical Conference and Exhibition, Dallas, Texas, 9-12 October.

30. Carlson, M.R., and Myer, J.W.: "The Effects of Retrograde Liquid Condensation on Single Well Productivity Determined Via Direct (Compositional) Modeling of A Hydraulic Fracture in a Low Permeability Reservoir," paper SPE 29561 presented at the 1995 SPE Rocky Mountain Regional/Low-Permeability Reservoirs Symposium, Denver, Colorado, 20-22 March.

31. Fussell, D.D.: "Single –Well Performance Predictions for Gas Condensate Reservoirs," *JPT* (July 1973) 860-870.

32. El-Banbi, A.H., McCain, W.D., and Semmelbeck, M.E.: "Investigation of Well Productivity in Gas-Condensate Reservoir," paper SPE 59773 presented at the 2000 SPE/CERI Gas Technology Symposium , Calgary, Canada, 3-5 April.

33. Cvetkovic, B., Economides, M.J., Omrcen, B., and Longaric, B.: "Production from Heavy Gas Condensate Reservoirs," paper SPE 20968 presented at the 1990 SPE European Petroleum Conference, Delft, The Netherlands, 21-24 October.

34. Sanger, P.J., and Hagoort, J.: "Recovery of Gas Condensate by Nitrogen Injection Compared with Methane Injection," *SPEJ* (July 1998) 26-36.

35. Gidley, J.L.: "A Method for Correcting Dimensionless Fracture Conductivity for Non-Darcy Flow Effects," paper SPE 20710 presented at the 1991 SPE Annual Technical Conference and Exhibition, New Orleans, Louisiana, 23-26 September.

36. Bartko, K.M., Nasr-El-Din, H.A., Rahim, Z., and Al-Muntasheri, G.A.: "Acid Fracturing of a Gas Carbonate Reservoir: The Impact of Acid Type and Lithology on Fracture Half Length and Width," paper SPE 84130 presented at the 2003 SPE Annual Technical Conference and Exhibition, Denver, Colorado, 5-8 October.

37. Ben-Naceur, K., and Economides, M.J.: "The Effectiveness of Acid Fractures and Their Production Behavior," paper SPE 18536 presented at the 1988 SPE Eastern Regional Meeting, Charleston, West Virginia, 1-4 November.

38. Settari, A.: "Modeling of Acid–Fracturing Treatments," *SPEPF* (Feb. 1993) 30-38.

39. Wang, X., Indriati, S., Valko, P.P., and Economides, M.J.: "Production Impartment and Purpose-Built Design of Hydraulic Fractures in Gas-Condensate Reservoirs," paper SPE 64749 presented at the 2000 SPE International Oil and Gas Conference and Exhibition, Beijing, China, 7-10 November.

APPENDIX A

FRACTURE GEOMETRY AND DIMENSIONLESS PARAMETER

TABLE A.1-SA-3, KHUFF-B RESERVOIR DATA						
Layer	Start of Interval	End of Interval	Thickness of interval	Permeability (md)	Porosity, %	Kh (md-ft)	Sg, %
1	10,872	10,882	10	0.68	8	6.8	70
2	10,890	10,900	10	0.68	8	6.8	82
3	10,905	10,925	20	0.89	11	17.8	82
4	10,942	10,952	10	0.53	6	5.3	75
5	10,976	10,986	10	0.82	10	8.2	70

TABLE A.2-SA-3, KHUFF-B AVERAGE RESERVOIR DATA AND WELL CHARACTERIZATION					
Parameter	Value	Unit	Parameter	Value	Unit
Net pay	60	ft	Reservoir Temperature	250	^{o}F
Permeability	0.75	md	Gas specific gravity	0.79	---
Growth thickness	114	ft	Reservoir pressure	7438	psi
Average porosity	8.6	---	Drainage area	2,224	acre
Average gas saturation	75.8	---	In-Situ Stress	10,895	psi
Viscosity	0.035	cp	Bottomhole flow pressure	---	psi

TABLE A.3- SA-3, KHUFF-B FRACTURE GEOMETRY AND DIMENSIONLESS PARAMETER				
Parameter	Symbol	Design Value	Calculated Value	Deviation %
Fracture Geometry				
Fracture half length, ft	x_f	447	447	---
Average width, in	w	0.096	0.17	40
Dimensionless fracture conductivity	C_{fD}	86	60	43
Effective conductivity, md-ft	kw_{af}	20,248	28,800	29
Results from Acid fracture Number Concept				
Acid fracture number	N_{af}	0.50	0.71	29
Dimensionless productivity Index	J_D	0.38	0.40	5

TABLE A.4-PUMPING SCHEDULE FOR SA-3, KHUFF-B

Stage Name	Slurry Rate (bbl/minute)	Pump Time (Minute)	Slurry Volume (bbl)	Acid Volume (gal)
Pad (polymer gel)/ Acid	41.6	10.3	428	12,597
Pad (polymer gel)/ Acid	48.9	9.4	459	13,514
Pad (VES)/ Acid	54.2	4	216	8,504
Pad (VES)/ Acid	56.5	5.6	316	12,411
Closed Fracture Acid	38.2	9.1	347	14,483

TABLE A.5-SA-3, KHUFF-C RESERVOIR DATA

Layer	Start of Interval	End of Interval	Thickness of interval	Permeability (md)	Porosity, %	Kh (md-ft)	Sg, %
1	11,366	11,376	10	1.81	12	18.1	83
2	11,390	11,410	20	1.05	9	21	72
3	11,446	11,456	10	3.49	17	34.9	77

TABLE A.6-SA-3, KHUFF-C AVERAGE RESERVOIR DATA AND WELL CHARACTERIZATION

Parameter	Value	Unit	Parameter	Value	Unit
Net pay	40	ft	Reservoir Temperature	253	^{o}F
Permeability	1.85	md	Gas specific gravity	0.79	---
Growth thickness	90	ft	Reservoir pressure	7,555	psi
Average porosity	12.6	---	Drainage area	2,224	acre
Average gas saturation	77.3	---	In-Situ Stress	11,400	psi
Viscosity	0.035	cp	Bottomhole flow pressure	---	psi

TABLE A.7- SA-3, KHUFF-C FRACTURE GEOMETRY AND DIMENSIONLESS PARAMETER				
Parameter	Symbol	Design Value	Calculated Value	Deviation %
Fracture Geometry				
Fracture half length, ft	x_f	408	408	---
Average width, in	w	0.16	0.23	30
Dimensionless fracture conductivity	C_{fD}	255	122	101
Effective conductivity, md-ft	kw_{af}	92,484	193,182	190
Results from Acid fracture Number Concept				
Acid fracture number	N_{af}	0.84	1.76	52
Dimensionless productivity Index	J_D	0.34	0.41	17

TABLE A.8-PUMPING SCHEDULE FOR SA-3, KHUFF-C				
Stage Name	Slurry Rate (bbl/minute)	Pump Time (Minute)	Slurry Volume (bbl)	Acid Volume (gal)
Pad (polymer gel)/ Acid	41.6	10.3	428	12,597
Pad (polymer gel)/ Acid	48.9	9.4	459	13,514
Pad (VES)/ Acid	54.2	4	216	8,504
Pad (VES)/ Acid	56.5	5.6	316	12,411
Closed Fracture Acid	38.2	9.1	347	14,483

TABLE A.9-SA-4 RESERVOIR DATA							
Layer	Start of Interval	End of Interval	Thickness of interval	Permeability (md)	Porosity, %	Kh (md-ft)	Sg, %
1	11,189	11,199	10	1.61	11.3	16.1	59
2	11,220	11,230	10	2.35	13.8	23.5	79
3	11,248	11,278	30	1.33	10.2	39.9	76
4	11,305	11,315	10	1.21	9.7	12.1	67
5	11,340	11,348	8	0.5	6.1	4	71

TABLE A.10-SA-4 AVERAGE RESERVOIR DATA AND WELL CHARACTERIZATION					
Parameter	**Value**	**Unit**	**Parameter**	**Value**	**Unit**
Net pay	68	ft	Reservoir Temperature	259	°F
Permeability	1.4	md	Gas specific gravity	0.73	---
Growth thickness	159	ft	Reservoir pressure	6,700	psi
Average porosity	10.22	---	Drainage area	2,224	acre
Average gas saturation	70.4	---	In-Situ Stress	11,178	psi
Viscosity	0.035	cp	Bottomhole flow pressure	---	psi

TABLE A.11- SA-4 FRACTURE GEOMETRY AND DIMENSIONLESS PARAMETER				
Parameter	**Symbol**	**Design Value**	**Calculated Value**	**Deviation %**
Fracture Geometry				
Fracture half length, ft	x_f	433	433	---
Average width, in	w	0.11	0.15	26
Dimensionless fracture conductivity	C_{fD}	24.2	22	10
Effective conductivity, md-ft	kw_{af}	12,972	14,741	12
Results from Acid fracture Number Concept				
Acid fracture number	N_{af}	0.17	0.19	10
Dimensionless productivity Index	J_D	0.38	0.39	2

TABLE A.12-PUMPING SCHEDULE FOR SA-4				
Stage Name	**Slurry Rate (bbl/minute)**	**Pump Time (Minute)**	**Slurry Volume (bbl)**	**Acid Volume (gal)**
Pad (polymer gel)/ Acid	35.8	12	429	12,630
Pad (polymer gel)/ Acid	50.6	8.5	430	12,644
Pad (VES)/ Acid	63	6.8	428	16,805
Pad (VES)/ Acid	61.1	6.9	421	16,538
Closed Fracture Acid	36.1	12.1	436	16,346

			TABLE A.13-SA-5 RESERVOIR DATA				
Layer	Start of Interval	End of Interval	Thickness of interval	Permeability (md)	Porosity, %	Kh (md-ft)	Sg, %
1	11,652	11,672	20	1.05	9	20	85
2	11,710	11,725	15	2.75	15	41	88
3	11,742	11,752	10	1.05	9	10	70

TABLE A.14-SA-5 AVERAGE RESERVOIR DATA AND WELL CHARACTERIZATION					
Parameter	Value	Unit	Parameter	Value	Unit
Net pay	45	ft	Reservoir Temperature	259	^{o}F
Permeability	1.6	md	Gas specific gravity	0.79	---
Growth thickness	100	ft	Reservoir pressure	6,400	psi
Average porosity	11	---	Drainage area	2,224	acre
Average gas saturation	81	---	In-Situ Stress	12,200	psi
Viscosity	0.035	cp	Bottomhole flow pressure	---	psi

TABLE A.15- SA-5 FRACTURE GEOMETRY AND DIMENSIONLESS PARAMETER				
Parameter	Symbol	Design Value	Calculated Value	Deviation %
Fracture Geometry				
Fracture half length, ft	x_f	354	354	---
Average width, in	w	0.15	0.23	34
Dimensionless fracture conductivity	C_{fD}	155	123	26
Effective conductivity, md-ft	kw_{af}	70,237	89,247	21
Results from Acid fracture Number Concept				
Acid fracture number	N_{af}	0.64	0.71	10
Dimensionless productivity Index	J_D	0.35	0.37	5

TABLE A.16-PUMPING SCHEDULE FOR SA-5				
Stage Name	Slurry Rate (bbl/minute)	Pump Time (Minute)	Slurry Volume (bbl)	Acid Volume (gal)
Pad (polymer gel)/ Acid	35	13.6	476	13,914
Pad (polymer gel)/ Acid	35	10.9	381.5	11,152
Pad (VES)/ Acid	45	5.3	238.5	9,355
Pad (VES)/ Acid	50	4.8	240	9,414
Closed Fracture Acid	35	9.1	318.5	13,243

APPENDIX B

DATA ANALYSIS

TABLE B.1-SUMMARY OF RESULTS OBTAINED FROM PERFPRM FOR SA-1				
Month	FWHP psig	Average Res. P. Psi	Skin	FBHP psi
1	4970	7469	-4.23	6442
2	4788	7436	-6.93	6410
3	4692	7402	-6.60	6278
4	4703	7370	-6.83	6278
5	4763	7357	-6.98	6344
6	4663	7325	-6.83	6278
7	4822	7296	-5.10	6312
8	4625	7272	-6.78	6179
9	4621	7250	-6.54	6179
10	4546	7218	-6.60	6147
11	4491	7188	-6.66	6081
12	4452	7155	-6.54	5981
13	4424	7124	-6.47	5949
14	4393	7093	-6.47	5949
15	4359	7060	-6.47	5883
16	4335	7030	-6.47	5816
17	4330	6998	-6.47	5839
18	3927	6971	-4.56	5349
19	3637	6943	-4.10	5003
20	3150	6918	-2.85	4428
21	3311	6895	-4.10	4687
22	3255	6865	-3.22	4543
23	3157	6840	-0.01	4400
24	3281	6833	-3.84	4629
25	3201	6807	-3.22	4485

TABLE B.2-SUMMARY OF RESULTS OBTAINED FROM PERFPRM FOR SA-2				
Month	FWHP psig	Average Res. P. Psi	Skin	FBHP psi
1	4502	7490	-5.40	5917
2	4362	7473	-4.94	5752
3	4080	7456	-4.94	5423
4	3960	7437	-4.56	5291
5	3893	7419	-4.10	5225
6	4067	7405	-3.55	5423
7	4110	7390	-3.84	5455
8	4100	7377	-3.84	5455
9	4009	7362	-3.55	5357
10	3843	7345	-5.40	5158
11	4495	7336	2.01	5917
12	4252	7326	-4.56	5620
13	4162	7314	-4.10	5522
14	3924	7299	-4.10	5259
15	3767	7283	-3.84	5060
16	3635	7266	-3.55	4896
17	3818	7252	-3.22	5126
18	3650	7238	-2.85	4928
19	3908	7225	-1.41	5225
20	3924	7215	-1.96	5259
21	N/A	N/A	N/A	N/A
22	4615	7208	-2.85	6047
23	4238	7199	-2.85	5620
24	3998	7188	-2.44	5323
25	4048	7178	-2.44	5357
26	4074	7168	-2.10	5340

TABLE B.3-LIST OF DIMENSIONLESS PRODUCTIVITY INDEX AT A GIVEN ACID NUMBER AND DIMENSIONLESS FRACTURE CONDUCTIVITY SA-1			
Month	N_{AC}	C_{FD}	J_D
1	0.202	34.054	0.375
2	0.198	33.432	0.375
3	0.184	30.983	0.374
4	0.184	30.983	0.374
5	0.191	32.184	0.375
6	0.184	30.983	0.374
7	0.187	31.596	0.375
8	0.173	29.264	0.374
9	0.173	29.264	0.374
10	0.170	28.729	0.374
11	0.164	27.657	0.374
12	0.155	26.108	0.373
13	0.152	25.631	0.373
14	0.152	25.631	0.373
15	0.146	24.674	0.373
16	0.141	23.740	0.373
17	0.143	24.056	0.373
18	0.107	18.137	0.370
19	0.088	14.858	0.368
20	0.063	10.667	0.363
21	0.073	12.384	0.365
22	0.068	11.398	0.364
23	0.062	10.496	0.362
24	0.071	11.977	0.364
25	0.065	11.023	0.363

TABLE B.4-LIST OF DIMENSIONLESS PRODUCTIVITY INDEX AT A GIVEN ACID NUMBER AND DIMENSIONLESS FRACTURE CONDUCTIVITY SA-2			
Month	N_{AC}	C_{FD}	J_D
1	0.097	13.837	0.379
2	0.089	12.582	0.377
3	0.073	10.408	0.374
4	0.068	9.646	0.372
5	0.065	9.286	0.372
6	0.073	10.408	0.374
7	0.075	10.602	0.374
8	0.075	10.602	0.374
9	0.071	10.020	0.373
10	0.063	8.934	0.371
11	0.097	13.837	0.379
12	0.082	11.660	0.376
13	0.078	11.019	0.375
14	0.067	9.469	0.372
15	0.059	8.443	0.369
16	0.054	7.682	0.367
17	0.062	8.771	0.370
18	0.055	7.825	0.368
19	0.065	9.286	0.372
20	0.067	9.469	0.372
21	N/A	N/A	N/A
22	0.105	14.913	0.380
23	0.082	11.660	0.376
24	0.069	9.825	0.373
25	0.071	10.020	0.373
26	0.070	9.922	0.373

APPENDIX C

CALCULATION SHEET

The entire data analysis generate in this work done in a separate Excel file for each field case.

VITA

NAME: Abdulwahab Al Ghamdi

PERMANENT ADDRESS: Saudi Aramco
                                         Dhahran, 31311
                                         P.O.Box, 8028
                                         Saudi Arabia

EDUCATION: B.S., Chemical Engineering (Cum Laude)
                                         King Fahd University of Petroleum and
                                         Minerals,
                                         Dhahran, Saudi Arabia
                                         October 2001

                                         M.S., Petroleum Engineering (Sponsored by
                                         Saudi Aramco)
                                         Texas A&M University, May 2006